



# Optimal plan and statistical inference for the inverse Nakagami-m distribution based on unified progressive hybrid censored data

Mohd Irfan , Anup Kumar Sharma\* 

*Department of Mathematics, National Institute of Technology Raipur, Raipur 492010, Chhattisgarh, India*

## Abstract

The present paper studies parametric inference for the inverse Nakagami-m distribution under a unified progressive hybrid censored sample. Maximum likelihood estimates of the unknown parameters are obtained using the Newton-Raphson method and the expectation-maximization algorithm. Approximate confidence intervals for the parameters are constructed via the variance-covariance matrix. Furthermore, Bayes estimates are investigated under the squared error and LINEX loss functions using gamma prior distributions for the unknown parameters. The Markov chain Monte Carlo approximation approach is employed to obtain the Bayes estimates and derive the highest posterior density credible intervals. The issue of hyperparameter selection is also discussed. In addition to Bayes estimates, maximum a posteriori estimates of the unknown parameters are computed using the Newton-Raphson method. The efficacy of the proposed approach is assessed through a Monte Carlo simulation study. The convergence of the MCMC sample is evaluated using various diagnostic plots. Three optimality criteria are presented to select the most suitable progressive scheme from different sampling plans. Two real-world applications that involve the fracture toughness of silicon nitride ( $\text{Si}_3\text{N}_4$ ) and the active repair times (in hours) for an airborne communication transceiver are used to illustrate the practical utility of the proposed methodology.

**Mathematics Subject Classification (2020).** 62F15, 65C05, 62F10, 62G05

**Keywords.** Bayesian estimation, expectation maximization, hybrid censoring, Nakagami-m distribution, optimality

## 1. Introduction

The Nakagami-m distribution introduced by Nakagami [22] is a probability distribution commonly used in wireless communication to model the fading characteristics of wireless channels. It is characterized by the shape parameter  $\nu$  and the scale parameter  $\eta$ . The Nakagami-m distribution is versatile, as it can represent a wide range of fading scenarios, from Rayleigh fading (when  $\nu = 1$ ) to Rician fading (when  $\nu > 1$ ). It finds applications

\*Corresponding Author.

Email addresses: irfan.maya786@gmail.com (M. Irfan), aksharma.ism@gmail.com (A.K. Sharma)

Received: 29.08.2024; Accepted: 09.05.2025

in various wireless communication systems, such as cellular networks, satellite communication, and underwater acoustic communication, where understanding and mitigating the effects of fading on signal transmission are crucial. By accurately modeling the fading phenomenon, the Nakagami-m distribution aids in designing robust communication systems, optimizing resource allocation, and enhancing overall system performance in challenging wireless environments.

The inverse distribution has improved understanding of the standard distribution and added flexibility for fitting data in various scientific and engineering domains, including reliability theory, finance and medical industries, and other areas.

In this article, we considered the inverse Nakagami-m distribution proposed by Louzada [10]. Let  $X$  be a non-negative random variable following the inverse Nakagami-m (INK) distribution with the cumulative distribution function (cdf) given by

$$F(x|\nu, \eta) = \frac{1}{\Gamma(\nu)} \Gamma\left(\nu, \frac{\nu}{\eta x^2}\right); x > 0, \nu > \frac{1}{2}, \eta > 0, \quad (1.1)$$

where  $\nu$  and  $\eta$  are the shape and scale parameters respectively. Henceforth, the INK distribution is represented as  $\text{INK}(\nu, \eta)$ . The probability distribution function (pdf) of the INK distribution is given by

$$f(x|\nu, \eta) = \frac{2}{\Gamma(\nu)} \left(\frac{\nu}{\eta}\right)^\nu x^{-2\nu-1} \exp\left(-\frac{\nu}{\eta x^2}\right); x > 0, \nu > \frac{1}{2}, \eta > 0. \quad (1.2)$$

**Proposition 1.1.** For the random variable  $X$  with the INK distribution, the  $r^{\text{th}}$  moment is given by

$$\mu_r = E[X^r] = \frac{1}{\Gamma(\nu)} \left(\frac{\nu}{\eta}\right)^{\frac{r}{2}} \Gamma\left(\nu - \frac{r}{2}\right), \text{ for } \nu > \frac{r}{2}. \quad (1.3)$$

**Proof.** We have

$$\begin{aligned} \mu_r &= \int_0^\infty x^r \frac{2}{\Gamma(\nu)} \left(\frac{\nu}{\eta}\right)^\nu x^{-2\nu-1} \exp\left(-\frac{\nu}{\eta x^2}\right) dx \\ &= \frac{2}{\Gamma(\nu)} \left(\frac{\nu}{\eta}\right)^\nu \int_0^\infty x^{2\left(\frac{r}{2}-\nu-\frac{1}{2}\right)} \exp\left(-\frac{\nu}{\eta x^2}\right) dx. \end{aligned} \quad (1.4)$$

Let  $x^2 = t$  and  $dx = \frac{dt}{2\sqrt{t}}$ , then

$$\mu_r = \frac{1}{\Gamma(\nu)} \left(\frac{\nu}{\eta}\right)^\nu \int_0^\infty t^{\left(\frac{r}{2}-\nu-1\right)} \exp\left(-\frac{\nu}{\eta t}\right) dt. \quad (1.5)$$

Again let  $\frac{\nu}{\eta t} = u$  and  $dt = -\frac{du}{u^2} \cdot \left(\frac{\nu}{\eta}\right)$ , then we have

$$\begin{aligned} \mu_r &= \frac{1}{\Gamma(\nu)} \left(\frac{\nu}{\eta}\right)^{\frac{r}{2}} \int_0^\infty u^{\nu-\frac{r}{2}-1} \exp(-u) du \\ &= \frac{1}{\Gamma(\nu)} \left(\frac{\nu}{\eta}\right)^{\frac{r}{2}} \Gamma\left(\nu - \frac{r}{2}\right), \text{ for } \nu > \frac{r}{2}. \end{aligned} \quad (1.6)$$

□

From the Equation (1.6) the mean and variance of Equation (1.2) are, respectively, given by

$$E[X] = \frac{1}{\Gamma(\nu)} \left(\frac{\nu}{\eta}\right)^{\frac{1}{2}} \Gamma\left(\nu - \frac{1}{2}\right), \text{ for } \nu > \frac{1}{2}, \quad (1.7)$$

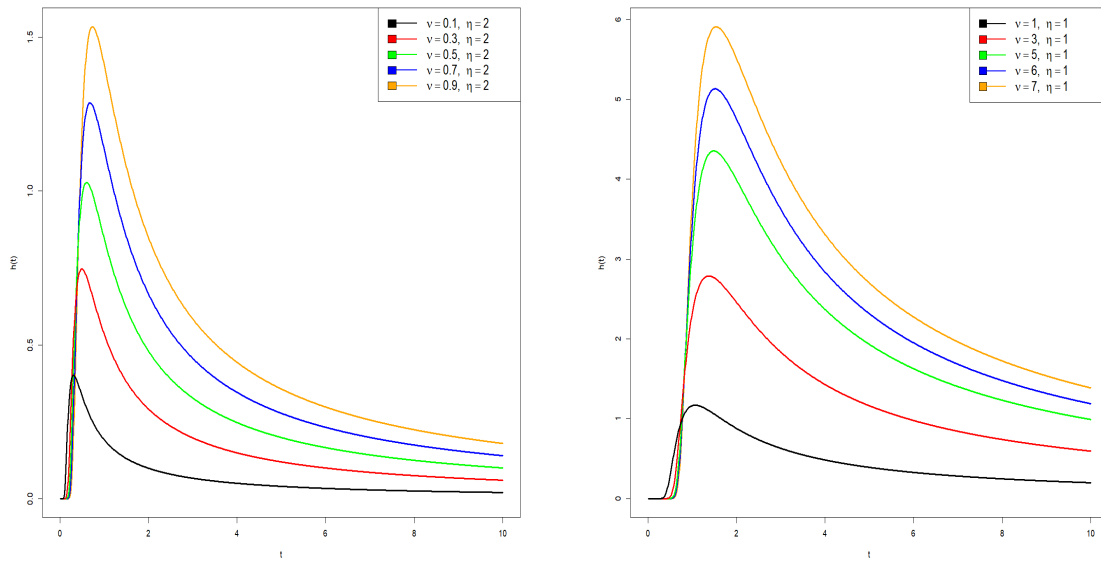


Figure 1. Hazard rate function of INK distribution.

and

$$\text{Var}[X] = \frac{\nu}{\eta} \left[ \frac{1}{\mu - 1} - \left\{ \frac{\Gamma(\mu - \frac{1}{2})}{\Gamma(\mu)} \right\}^2 \right], \mu > 1. \tag{1.8}$$

The reliability and hazard rate function (hrf) of the INK distribution at time t are obtained as follows:

$$R(t) = \frac{1}{\Gamma(\nu)} \gamma \left( \nu, \frac{\nu}{\eta t^2} \right); t > 0 \tag{1.9}$$

and

$$H(t) = 2 \left( \frac{\nu}{\eta} \right)^\nu t^{-2\nu-1} \exp \left( -\frac{\nu}{\eta t^2} \right) \gamma \left( \nu, \frac{\nu}{\eta t^2} \right)^{-1}, \tag{1.10}$$

where  $\Gamma(\cdot, \cdot)$  and  $\gamma(\cdot, \cdot)$  represent the incomplete upper and lower gamma functions, respectively [21].

Louzada [10] analyzed the nature of the hrf in Equation (1.10) and investigated that the hazard rate function of the INK distribution is unimodal for all  $\nu > 0$  and  $\eta > 0$ . Figure 1 depicts the pictorial representation of the INK distribution. From Figure 1, it is observed that the INK failure process indicates an increase in its hazard in the early stage of the process, and after reaching its mode, quickly decreases as time increases. This type of statistical model is used in diverse fields, such as product reliability, medical prognosis, cybersecurity, environmental studies, insurance risk assessment, industrial process control, and consumer behavior analysis. For example, in product reliability, this model helps assess early failures in electronics, where defects cause high initial hazards that drop as defective units are identified and resolved. Similarly, in the medical prognosis, it can predict postoperative complications, with the highest risk immediately after surgery that decreases as patients recover. Cybersecurity identifies peak vulnerability periods following new software releases, which decrease as patches are implemented. Environmental studies use it to understand the survival rates of reintroduced species, which face high initial mortality that reduces over time. Insurance companies apply it to assess new policyholders'

risk, and industries use it to monitor machinery breakdowns, which are frequent during initial setup but decline as processes stabilize. Finally, consumer behavior analysis helps us to understand the customer churn of new subscribers, which is high initially, but decreases as they engage more with the service. As a result, this model can be applied when we quickly witness high-intensity failure and some failure that occurs very far from the mode.

Several two-parameter lifetime distributions with flexible hrfs have been proposed recently, expanding the range of available models for reliability studies. Notable examples include the new two-parameter lifetime distribution introduced by Hashem pour [12], which exhibits various shapes of the hazard rate, and the mixture of exponential and Weibull distributions proposed by Mohammad [20], which balances the simplicity of the exponential model with the flexibility of the Weibull distribution. Furthermore, the weighted G family of probability distributions developed by Shaheed [31] provides an adaptable framework for data modeling over time and has shown strong performance in reliability applications. Although these flexible distributions offer alternative modeling approaches, our study focuses on the INK distribution because of its superior performance in real-world failure data modeling. Specifically, we demonstrate its effectiveness in the context of unified progressive hybrid censored data, highlighting its ability to capture failure characteristics accurately.

In reliability theory, censored data is a strategic asset that allows researchers to gain valuable insights into system reliability and survival characteristics while optimizing time and cost. By strategically truncating data collection at predefined points, such as the completion of a study period or after a certain number of events, censored data enables efficient analysis without compromising the validity of results. This approach accelerates the research process and minimizes resource expenditure, making it a cornerstone of cost-effective reliability studies. Through censored data analysis, researchers can extract meaningful conclusions regarding failure patterns, maintenance strategies, and system performance, empowering decision makers with actionable insights while maximizing time and cost efficiency in reliability analysis.

Numerous censoring schemes exist in the literature. For example, Epstein [5] investigated the hybrid censoring scheme (HCS), a combination of type-I and type-II censoring schemes. One can consult Balakrishnan and Aggarwala [26] for in-depth discussions on type-I and type-II censoring schemes. Child *et al.* [1] suggested the type-II HCS and Chandrasekar *et al.* [4] proposed the generalized type-I and type-II censoring scheme (GT-IHCS & GT-IIHCS). These censoring schemes were introduced to avoid the disadvantages of the type-I and type-II HCS. However, these two censoring schemes have some drawbacks, too. In the case of GT-IIHCS, the experimenter may not have the  $m^{\text{th}}$  failure due to the pre-fix time. However, with the GT-IIHCS, it is possible to obtain an effective sample size that is zero or very small. To address these drawbacks, Balakrishnan *et al.* [27] suggested the unified hybrid censoring systems of type I and type II (UHCS). Within this scheme, two thresholds  $T_1$  and  $T_2$  such that  $0 < T_1 < T_2$  are predefined, together with two numbers,  $k$  and  $m$ , where  $k < m \leq n$ . Similarly to HCS, UHCS has a drawback. The UHCS lacks the adaptability to remove experimental units before the experiment is ended. Gorny and Cramer [13] proposed a unified progressive hybrid censoring scheme (UPHCS) to prevent such situations.

The procedures involved in UPHCS can be described as follows: Consider that there are  $n$  items in the experiment. Assume that they are independently and identically distributed with pdf  $f(x)$  and cdf  $F(x)$ . Before starting the experiments, we give two integers  $k$  and  $m$ , where  $k < m \leq n$  and a progressive censoring scheme  $R_1, R_2, \dots, R_m$ , where  $R_m = n - m - \sum_{i=1}^{m-1} R_i$  and  $R_i \geq 0$ . In the course of the experiment, if the  $i^{\text{th}}$  failure, whose lifetime is represented by  $X_{i:m:n}$ , then  $R_i$  items are withdrawn from the live items in the experiment. As the experiment continues,  $R_i$  might have a different value. However, there are two thresholds  $T_1$  and  $T_2$  ( $T_1, T_2 \in (0, \infty)$ ) with  $T_1 < T_2$ , which are pre-specified

and fixed. When the test reaches  $T_1$ , it indicates that it needs to be accelerated. The experiment is allowed to proceed. The second threshold,  $T_2$ , denotes the longest time that the experiment will allow. The experiment must end at  $T_2$  regardless of whether the failure samples reach the target number  $m$ . Four cases were used in the experiment; the specifics are listed below:

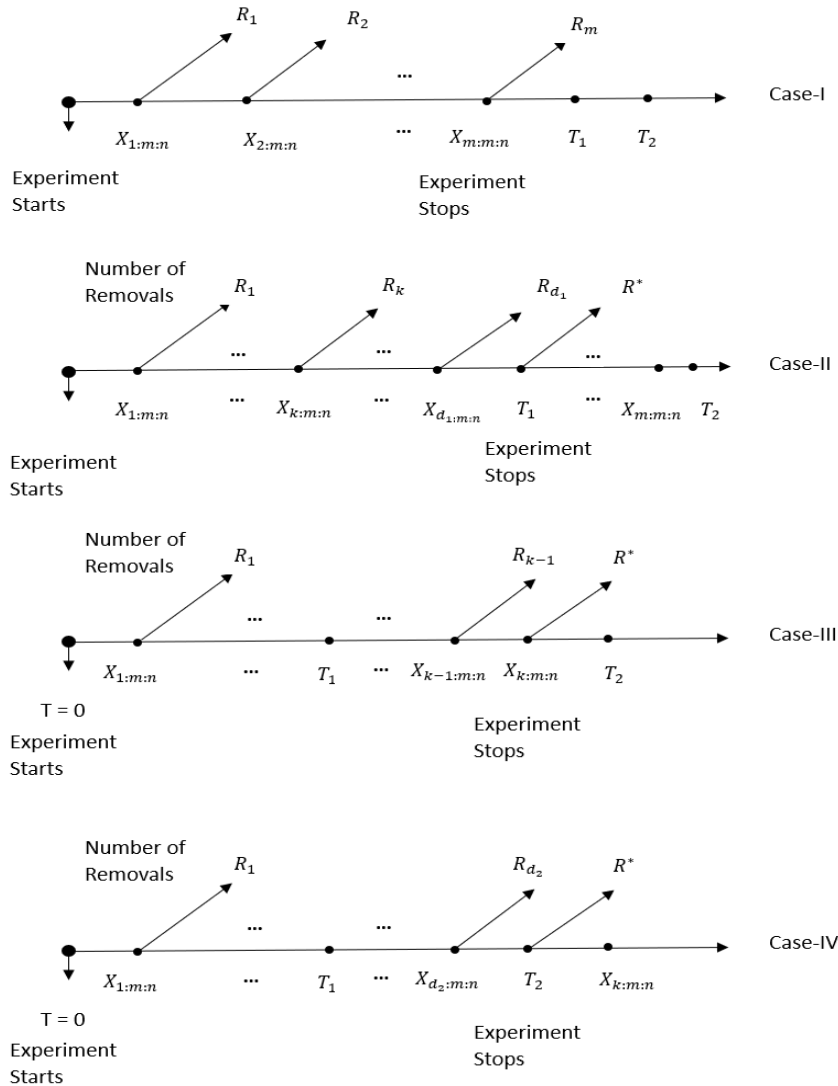


Figure 2. Schematic representation of UPHC sample.

- **Case I:**  $X_{1:m:n}, \dots, X_{m:m:n}$ , if  $X_{m:m:n} < T_1$ ;
- **Case II:**  $X_{1:m:n}, \dots, X_{k:m:n}, \dots, X_{d_1:m:n}$ , if  $X_{k:m:n} < T_1 < X_{m:m:n}$ ;
- **Case III:**  $X_{1:m:n}, \dots, X_{k:m:n}$ , if  $T_1 < X_{k:m:n} < T_2$ ;
- **Case IV:**  $X_{1:m:n}, \dots, X_{d_2:m:n}$ , if  $T_2 < X_{m:m:n}$ ,

where  $d_1$  and  $d_2$  represents the number of failure items before the threshold time  $T_1$  and  $T_2$ . The schematic representation of the UPHC scheme is shown in Figure 2.

The primary benefit of the UPHC scheme is that it guarantees that the test duration will not exceed  $T_2$ , thus resolving the issue where GHCS cannot guarantee the test duration. Furthermore, we can set  $T_2$  to a very large value, which means that the experiment can

continue without limitations if we are more concerned with the adequate sample size than with the test time.

The UPHC schemes are especially useful in real-life applications where time, cost, or resource constraints must be balanced with the need for informative data. For example, in reliability testing of complex electronic systems, it is often necessary to remove some surviving units at various stages (progressive censoring) to minimize operational costs. Moreover, regulatory bodies can impose a maximum allowed test duration to ensure safety and compliance. The dual-threshold mechanism of UPHC (with  $T_1$  and  $T_2$ ) allows for such flexibility. Similar situations arise in biomedical studies, accelerated life testing, and industrial product validation, where such censoring strategies help manage logistical and ethical constraints while ensuring sufficient data is collected for inference. (See, Balakrishnan *et al.* [27] and Gorny and Cramer [13]).

To the best of our knowledge, Kim and Lee [15] were the first to address the estimation problems for the Weibull distribution under a UPHC sample. Lone *et al.* [32] explored parameter estimation and the optimal design for the gamma-mixed Rayleigh model under the UPHC sample. Dutta and Kayal [34] conducted statistical inference for the Burr-III distribution using UPHC data. However, recent studies have not investigated the inferential aspects of the INK lifetime model under the newly introduced UPHC sample. It is noted that the INK distribution fits various real-world datasets better than the Burr-III, inverse Weibull, inverse Gompertz, and inverse Rayleigh distributions. For example, the INK distribution fits the failure time of mechanical devices in an aircraft, the failure time of an agricultural machine [10] and the fracture toughness of silicon nitrate [34]. Recently, Wang *et al.* [17] discussed the parameter estimation of the INK distribution under a progressive type-II censored sample.

To our knowledge, no research has been done on estimating the parameters of the INK distribution in the presence of data derived from the UPHC sample. Therefore, to address this void, our study aims to employ frequentist and Bayesian approaches to obtain both points and interval estimates of the unknown model parameters of the INK distribution under the UPHC sample. In the frequentist approach, the maximum likelihood estimates (MLE) are computed using the Newton-Raphson method and the expectation maximization (EM) algorithm. Approximate confidence intervals (ACIs) for unknown parameters are obtained via a variance-covariance matrix. The MCMC approximation techniques, such as the Metropolis-Hastings (M-H) algorithm, have been adopted in the Bayesian approach. Further, the highest posterior density credible interval is created. In addition to Bayes estimates, maximum a posteriori (MAP) estimates are investigated using Newton-Rapson methods. To show the effectiveness of the proposed estimates, a simulation study is performed using mean square error (MSE), absolute bias (AB), average confidence length (ACL), and coverage probabilities (CPs). Moreover, several optimality criteria have been proposed to investigate the optimal censoring scheme. A real-life data set is also analyzed to demonstrate the practical applicability of the suggested method in a real-world scenario. The highlights of the findings of this study are given as follows: Firstly, two classical estimation techniques such as likelihood as well as expectation maximization have been employed to estimate the parameters of the INK distribution under UPHC sample. In addition, approximate confidence intervals for the parameters of the INK distribution under the UPHC sample are also obtained. Secondly, Bayes estimates for the parameters have been derived using maximum a posteriori and MCMC techniques under SELF and LLF along with HPD credible intervals. Finally, we have obtained the optimal progressive censoring plan using three different optimality criteria.

The rest of this paper is structured as follows: Section 2 obtains the estimate of the points and intervals of the unknown model parameters based on the UPHC sample using MLEs using the Newton Rapson method and the EM algorithm. Section 3 presents the derivation of Bayesian estimation along with the HPD credible intervals. Section 4 obtains

the MAP estimates of the unknown parameters. Section 5 is dedicated to executing a Monte Carlo simulation study. Section 6 discusses various optimality criteria for choosing an optimal progressive censoring plan. Section 7 delves into the analysis of a real-life data set to confirm the practical applicability of the proposed techniques. The convergence of the MCMC sample was also tested using different diagnostic plots. Finally, the paper concludes in Section 8.

## 2. Inference

In this section, the MLE of the unknown parameters of the INK distribution is obtained by the Newton-Rapson method and the EM algorithm. In addition, the ACI of the unknown parameters is derived.

### 2.1. Maximum likelihood estimation

This section focused on the estimation of unknown parameters of the INK distribution using MLE procedures based on the UPHC sample. Assume that  $X_{1:m:n}, \dots, X_{D:m:n}$  are UPHC sample from the INK distribution. Throughout the paper, denote data =  $x_1, \dots, x_D$ , where  $x_i = x_{i:m:n}$ ,  $i = 1, \dots, D$ . The likelihood function based on the compact form can be written as follows:

$$L(\nu, \eta | X) \propto \left( \frac{2}{\Gamma(\nu)} \right)^D \left( \frac{\nu}{\eta} \right)^{\nu D} \prod_{i=1}^D x_i^{-2\nu-1} e^{-\frac{\nu}{\eta x_i^2}} \left[ \frac{1}{\Gamma(\nu)} \gamma \left( \nu, \frac{\nu}{\eta x_i^2} \right) \right]^{R_i} \left[ \frac{1}{\Gamma(\nu)} \gamma \left( \nu, \frac{\nu}{\eta T^2} \right) \right]^{R^*}, \quad (2.1)$$

where

$$D = \begin{cases} m, & \text{case I} \\ d_1, & \text{case II} \\ k, & \text{case III} \\ d_2, & \text{case IV} \end{cases}, T = \begin{cases} x_m, & \text{case I} \\ T_1, & \text{case II} \\ x_k, & \text{case III} \\ T_2, & \text{case IV} \end{cases},$$

Here, T is the time at which the experiment stopped and  $R^* = n - D - \sum_{i=1}^D R_i$ . Thus, the log-likelihood function up to a proportionality constant can be expressed as follows:

$$l(\nu, \eta | data) = D \log \left( \frac{2}{\Gamma(\nu)} \right) + \nu D \log \left( \frac{\nu}{\eta} \right) - (2\nu + 1) \sum_{i=1}^D \log(x_i) - \frac{\nu}{\eta} \sum_{i=1}^D \frac{1}{x_i^2} + \sum_{i=1}^D R_i \log \left[ \frac{\gamma \left( \nu, \frac{\nu}{\eta x_i^2} \right)}{\Gamma(\nu)} \right] + R^* \log \left[ \frac{\gamma \left( \nu, \frac{\nu}{\eta T^2} \right)}{\Gamma(\nu)} \right]. \quad (2.2)$$

The likelihood function provided in Equation (2.2) can be maximized to obtain the MLEs of  $\nu$  and  $\eta$ . Taking the partial derivative of  $l(\nu, \eta)$  given in equation (2.2) with respect to  $\nu$  and  $\eta$ , the likelihood equations can be stated as follows:

$$\begin{aligned} \frac{\partial l}{\partial \nu} = & -D \frac{\Gamma(\nu)'}{\Gamma(\nu)} + D \log\left(\frac{\nu}{\eta}\right) + \eta D - 2 \sum_{i=1}^D \log(x_i) - \frac{1}{\eta} \sum_{i=1}^D \frac{1}{x_i^2} + \sum_{i=1}^D R_i \frac{\gamma_\nu\left(\nu, \frac{\nu}{\eta x_i^2}\right)'}{\gamma\left(\nu, \frac{\nu}{\eta x_i^2}\right)} \\ & - \sum_{i=1}^D R_i \frac{\Gamma(\nu)'}{\Gamma(\nu)} + R^* \frac{\gamma_\nu\left(\nu, \frac{\nu}{\eta T^2}\right)'}{\gamma\left(\nu, \frac{\nu}{\eta T^2}\right)} - R^* \frac{\Gamma(\nu)'}{\Gamma(\nu)}, \end{aligned} \tag{2.3}$$

and

$$\frac{\partial l}{\partial \eta} = -\frac{D\nu}{\eta} + \frac{\nu}{\eta^2} \sum_{i=1}^D \frac{1}{x_i^2} + \sum_{i=1}^D R_i \frac{\gamma_\eta\left(\nu, \frac{\nu}{\eta x_i^2}\right)'}{\gamma\left(\nu, \frac{\nu}{\eta x_i^2}\right)} + R^* \frac{\gamma_\eta\left(\nu, \frac{\nu}{\eta T^2}\right)'}{\gamma\left(\nu, \frac{\nu}{\eta T^2}\right)}, \tag{2.4}$$

where  $\Gamma(\nu)'$  is the digamma function,  $\gamma_\nu(\cdot, \cdot)'$  and  $\gamma_\eta(\cdot, \cdot)'$  represents the derivative of the lower incomplete gamma function with respect to  $\nu$  and  $\eta$  respectively. It is noted that (2.3) and (2.4) cannot be solved directly. Using a non-linear optimization technique, the non-linear system of equations provided by (2.3) and (2.4) must be numerically solved to obtain the MLE of  $\nu$  and  $\eta$ , respectively, denoted as  $\hat{\nu}$  and  $\hat{\eta}$ . Notable is the fact that the MLEs of the parameters were calculated using the R software's 'nleqslv' package.

Researchers have paid considerable attention to studying the existence and unique properties of MLEs in terms of statistical inference. However, it is not always possible to derive the existence and uniqueness property of MLE of the parameters because of the complicated expression of the second order of the log-likelihood function. To overcome this problem graphically, a contour plot of the log-likelihood function becomes useful. In our case, studying the second-order partial derivative of the log-likelihood function with respect to  $\nu$  and  $\eta$  is difficult. Therefore, the contour plot of the MLE for the parameters  $\nu$  and  $\eta$  are presented in Figure 3. This plot suggests that MLEs may exist uniquely.

### 2.2. Expectation-Maximization algorithm

The EM method is a robust iterative algorithm used for estimating parameters in statistical models, mainly when dealing with incomplete or latent data. It alternates between an Expectation (E) step, where it computes the expected value of missing data given the observed data and current parameter estimates, and a Maximization (M) step, where it updates the parameters to maximize the likelihood of the observed data, incorporating the expected values obtained from the E-step. EM is widely applied in various fields due to its ability to handle missing data and its effectiveness in parameter estimation tasks such as clustering, density estimation, and hidden Markov models. In this section, we consider the problems of estimating the INK parameters as a problem of incomplete data [3]. Assume that  $X = (X_1, \dots, X_D)$  is an observed sample,  $(Z = Z_1, \dots, Z_D)$  is an unobserved sample, where  $Z_r = (Z_{r1}, \dots, Z_{rR_r})$ ,  $r = 1, 2, \dots, D$  is a vector  $1 \times R_r$   $Z' = (Z'_1, \dots, Z'_{R^*})$  as a censored sample. The complete data set can be modeled as  $Y = (X, Z, Z')$  and the corresponding log-likelihood function can be expressed as

$$l_c(\theta) = n \log \left( \frac{2}{\Gamma(\nu)} \right) + \nu n \log \left( \frac{\nu}{\eta} \right) - (2\nu + 1) \sum_{i=1}^D \log(x_i) - \frac{\nu}{\eta} \sum_{i=1}^D \frac{1}{x_i^2} - (2\nu + 1) \sum_{i=1}^D \sum_{j=1}^{R_j} \log(Z_{ij}) - \frac{\nu}{\eta} \sum_{i=1}^D \sum_{j=1}^{R_j} \left( \frac{1}{Z_{ij}^2} \right) - (2\nu + 1) \sum_{i=1}^{R^*} \log(Z_{T_j}) - \frac{\nu}{\eta} \sum_{i=1}^{R^*} \left( \frac{1}{Z_{T_j}^2} \right).$$

Using the algorithm's E-step, it can be seen that

$$\begin{aligned} l_c = & n \log \left( \frac{2}{\Gamma(\nu)} \right) + \nu n \log \left( \frac{\nu}{\eta} \right) - (2\nu + 1) \sum_{i=1}^D \log(x_i) - \frac{\nu}{\eta} \sum_{i=1}^D \left( \frac{1}{x_i^2} \right) \\ & - (2\nu + 1) \sum_{i=1}^D \sum_{j=1}^{R_j} E(\log(Z_{ij}) | Z_{ij} > x_i) - \frac{\nu}{\eta} \sum_{i=1}^D \sum_{j=1}^{R_j} E \left( \frac{1}{Z_{ij}^2} | Z_{ij} > x_i \right) \\ & - (2\nu + 1) \sum_{j=1}^{R^*} E(\log(Z_{T_j}) | Z_{T_j} > T) - \frac{\nu}{\eta} \sum_{j=1}^{R^*} E \left( \frac{1}{Z_{T_j}^2} | Z_{T_j} > T \right), \end{aligned} \quad (2.5)$$

where

$$\begin{aligned} E(\log(Z_{ij}) | Z_{ij} > x_i) &= \int_{x_i}^{\infty} \frac{f(t; \nu, \eta)}{1 - F(x_i; \nu, \eta)} \log(t) dt \\ &= \frac{1}{1 - F(x_i; \nu, \eta)} \frac{2}{\Gamma(\nu)} \left( \frac{\nu}{\eta} \right)^\nu \int_{x_i}^{\infty} t^{-(2\nu+1)} \exp \left( -\frac{\nu}{\eta t^2} \right) \log(t) dt \\ &= A(x_i; \nu, \eta), \end{aligned}$$

$$\begin{aligned} E \left( \frac{1}{Z_{ij}^2} | Z_{ij} > x_i \right) &= \frac{2}{\Gamma(\nu)} \left( \frac{\nu}{\eta} \right)^\nu \frac{1}{1 - F(x_i; \nu, \eta)} \int_{x_i}^{\infty} t^{-(2\nu+1)} \exp \left( -\frac{\nu}{\eta t^2} \right) \cdot \frac{1}{t^2} dt \\ &= B(x_i; \nu, \eta), \end{aligned}$$

and

$$\begin{aligned} E(\log(Z_{T_j}) | Z_{T_j} > T) &= \frac{2}{\Gamma(\nu)} \left( \frac{\nu}{\eta} \right)^\nu \frac{1}{1 - F(T; \nu, \eta)} \int_T^{\infty} t^{-(2\nu+1)} \exp \left( -\frac{\nu}{\eta t^2} \right) \cdot \log(t) dt \\ &= C(T; \nu, \eta), \end{aligned}$$

$$\begin{aligned} E \left( \frac{1}{Z_{T_j}^2} | Z_{T_j} > T \right) &= \frac{2}{\Gamma(\nu)} \left( \frac{\nu}{\eta} \right)^\nu \frac{1}{1 - F(T; \nu, \eta)} \int_T^{\infty} t^{-(2\nu+1)} \exp \left( -\frac{\nu}{\eta t^2} \right) \cdot \frac{1}{t^2} dt \\ &= D(T; \nu, \eta). \end{aligned}$$

Thus, the log-likelihood can be expressed as

$$\begin{aligned} l_c = & n \log \left( \frac{2}{\Gamma(\nu)} \right) + \nu n \log \left( \frac{\nu}{\eta} \right) - (2\nu + 1) \sum_{i=1}^D \log(x_i) - \frac{\nu}{\eta} \sum_{i=1}^D \frac{1}{x_i^2} \\ & - (2\nu + 1) \sum_{i=1}^D R_i A(x_i; \nu, \eta) - \frac{\nu}{\eta} \sum_{i=1}^D R_i B(x_i; \nu, \eta) \\ & - (2\nu + 1) R^* C(T; \nu, \eta) - \frac{\nu}{\eta} R^* D(T; \nu, \eta). \end{aligned} \quad (2.6)$$

The log-likelihood function provided in Equation (2.6) will now be maximized in M-step with respect to  $\nu$  and  $\eta$ . We must solve the following equation to obtain the updated  $(k + 1)^{th}$  iteration of  $\eta$  for the provided  $k^{th}$  iteration.

$$\hat{\eta} = \frac{\sum_{i=1}^D \frac{1}{x_i^2} + \sum_{i=1}^D R_i B(x_i; \nu_{(k)}, \eta_{(k)}) + R^* D(T; \nu_{(k)}, \eta_{(k)})}{n}. \tag{2.7}$$

The corresponding updated  $\nu$  can be calculated as follows using the revised estimations of  $\eta$ .

$$\begin{aligned} n \frac{\Gamma(\nu)'}{\Gamma(\nu)} - n(\log(\nu) + 1) + n \log(\hat{\eta}) + 2 \sum_{i=1}^D \log(x_i) + \frac{1}{\hat{\eta}} \sum_{i=1}^D \frac{1}{x_i^2} + 2 \sum_{i=1}^D R_i A(x_i; \nu_{(k)}, \eta_{(k)}) \\ + \frac{1}{\hat{\eta}} \sum_{i=1}^D R_i B(x_i; \nu_{(k)}, \eta_{(k)}) + 2R^* C(T; \nu_{(k)}, \eta_{(k)}) + \frac{1}{\hat{\eta}} R^* D(T; \nu_{(k)}, \eta_{(k)}) = 0. \end{aligned} \tag{2.8}$$

This iterative process of E-step and M-step will be repeated until the desired accuracy is attained in order to produce the estimations of  $\nu$  and  $\eta$ .

### 2.3. Approximate confidence intervals

This section deals with constructing frequentist confidence intervals (CIs) of the unknown parameters of the INK distribution. The  $100(1 - \psi)\%$  ACIs of  $\nu$  and  $\eta$  under MLE are derived using the asymptotic variance and covariance matrix (V-C) for the corresponding MLEs. Approximate CIs using the Fisher information matrix (FIM) involve computing the inverse of the FIM and using it to construct CIs for the parameters. The inverse of the FIM approximates the covariance matrix of the parameter estimates, assuming the likelihood function is well behaved and the MLE is approximately normally distributed.

By differentiating Equations (2.3) and (2.4) partially with respect to  $\nu$  and  $\eta$ , the observed FIM evaluated at their MLEs is defined as follows:

$$I_{ij}(\theta) = E \left[ -\frac{\partial^2 l(\theta|x)}{\partial \theta^2} \right], \quad i, j = 1, 2; \theta = (\hat{\nu}, \hat{\eta}).$$

Obtaining the exact solution for the expectation in the above equation is cumbersome. Thus, the approximate variance and covariance matrix,  $I^{-1}(\hat{\theta})$ , for the MLEs  $\hat{\theta}$ , is given by

$$I^{-1}(\hat{\nu}, \hat{\eta}) \cong \begin{bmatrix} -\frac{\partial^2 l}{\partial \nu^2} & -\frac{\partial^2 l}{\partial \nu \partial \eta} \\ -\frac{\partial^2 l}{\partial \eta \partial \nu} & -\frac{\partial^2 l}{\partial \eta^2} \end{bmatrix}^{-1} = \begin{bmatrix} var(\hat{\nu}) & cov(\hat{\nu}, \hat{\eta}) \\ cov(\hat{\nu}, \hat{\eta}) & var(\hat{\eta}) \end{bmatrix}, \tag{2.9}$$

where

$$\begin{aligned} \frac{\partial^2 l}{\partial \nu^2} = -D \frac{\Gamma(\nu)'' \Gamma(\nu) - (\Gamma(\nu)')^2}{(\Gamma(\nu))^2} + \frac{D}{\nu} + \sum_{i=1}^D R_i \frac{\gamma_\nu \left( \nu, \frac{\nu}{\eta x_i^2} \right)'' \gamma \left( \nu, \frac{\nu}{\eta x_i^2} \right) - \left[ \gamma_\nu \left( \nu, \frac{\nu}{\eta x_i^2} \right) \right]'^2}{\left[ \gamma \left( \nu, \frac{\nu}{\eta x_i^2} \right) \right]^2} \\ + R^* \frac{\gamma_\nu \left( \nu, \frac{\nu}{\eta T^2} \right)'' \gamma \left( \nu, \frac{\nu}{\eta T^2} \right) - \left[ \gamma_\nu \left( \nu, \frac{\nu}{\eta T^2} \right) \right]'^2}{\left[ \gamma \left( \nu, \frac{\nu}{\eta T^2} \right) \right]^2}, \end{aligned} \tag{2.10}$$

$$\begin{aligned} \frac{\partial^2 l}{\partial \eta^2} &= \frac{D\nu}{\eta^2} - \frac{2\nu}{\eta^3} \sum_{i=1}^D \frac{1}{x_i^2} + \sum_{i=1}^D R_i \frac{\gamma_\eta \left( \nu, \frac{\nu}{\eta x_i^2} \right)'' \gamma \left( \nu, \frac{\nu}{\eta x_i^2} \right) - \left[ \gamma_\eta \left( \nu, \frac{\nu}{\eta x_i^2} \right)' \right]^2}{\left[ \gamma \left( \nu, \frac{\nu}{\eta x_i^2} \right) \right]^2} \\ &+ R^* \frac{\gamma_\eta \left( \nu, \frac{\nu}{\eta T^2} \right)'' \gamma \left( \nu, \frac{\nu}{\eta T^2} \right) - \left[ \gamma_\eta \left( \nu, \frac{\nu}{\eta T^2} \right)' \right]^2}{\left[ \gamma \left( \nu, \frac{\nu}{\eta T^2} \right) \right]^2}, \end{aligned} \quad (2.11)$$

and

$$\begin{aligned} \frac{\partial^2 l}{\partial \nu \partial \eta} &= \frac{\partial^2 l}{\partial \eta \partial \nu} = -\frac{D}{\eta} + \frac{1}{\eta} \sum_{i=1}^D \frac{1}{x_i^2} + \sum_{i=1}^D R_i \frac{\gamma_{\nu\eta} \left( \nu, \frac{\nu}{\eta x_i^2} \right)'' \gamma \left( \nu, \frac{\nu}{\eta x_i^2} \right) - \left[ \gamma_\eta \left( \nu, \frac{\nu}{\eta x_i^2} \right)' \right]^2}{\left[ \gamma \left( \nu, \frac{\nu}{\eta x_i^2} \right) \right]^2} \\ &+ R^* \frac{\gamma_{\nu\eta} \left( \nu, \frac{\nu}{\eta T^2} \right)'' \gamma \left( \nu, \frac{\nu}{\eta T^2} \right) - \left[ \gamma_\eta \left( \nu, \frac{\nu}{\eta T^2} \right)' \right]^2}{\left[ \gamma \left( \nu, \frac{\nu}{\eta T^2} \right) \right]^2}. \end{aligned} \quad (2.12)$$

Thus, the  $100(1-\psi)\%$  ACIs for the unknown model parameters are obtained respectively as

$$\hat{\nu} \pm z_{\frac{\psi}{2}} \sqrt{\text{var}(\hat{\nu})} \quad \text{and} \quad \hat{\eta} \pm z_{\frac{\psi}{2}} \sqrt{\text{var}(\hat{\eta})},$$

respectively, where  $z_{\frac{\psi}{2}}$  denote the upper  $\frac{\psi}{2}$ <sup>th</sup> percentile of the standard normal distribution.

### 3. Bayesian Inference

This section focuses on deriving the Bayes estimates (BEs) of unknown parameters  $\nu$  and  $\eta$  for the INK distribution based on the UPHC sample. In Bayesian estimation, loss functions are employed to quantify the discrepancy between true parameter values and their estimates. Two types of loss function occur mainly in nature: symmetric and asymmetric. Symmetric loss functions, such as the squared error loss function (SELF), treat overestimation and underestimation symmetrically, penalizing deviations equally in either direction. These are frequently used when the cost of overestimating is thought to be equally as high as that of underestimating. On the other hand, asymmetric loss functions, such as the LINEX loss function (LLF), represent scenarios in which the effects of estimation errors are uneven by assigning different penalties to overestimation and underestimation. Here, two types of loss function are considered: SELF and LLF. These two loss functions are defined as follows:

$$L_{SELF}(\zeta, \hat{\zeta}) = (\zeta - \hat{\zeta})^2, \quad (3.1)$$

$$L_{LLF}(\zeta, \hat{\zeta}) = e^{h(\zeta - \hat{\zeta})} - h(\zeta - \hat{\zeta}) - 1; h \neq 0, \quad (3.2)$$

where  $\hat{\zeta}$  is estimated value of  $\zeta$ . To derive the Bayes estimator, it is necessary to have prior distributions for the unknown model parameters. The prior distribution serves as a crucial element by encoding existing knowledge or beliefs about the parameters before observing new data. In this context, we examine the utilization of independent gamma prior distributions for the unknown parameters  $\nu$  and  $\eta$ , characterized by hyperparameters  $(a_1, b_1)$  and  $(a_2, b_2)$ , correspondingly. The joint prior PDF of  $\nu$  and  $\eta$  can be obtained as

$$\pi(\nu, \eta) \propto \nu^{a_1-1} \exp(-b_1\nu) \eta^{a_2-1} \exp(-b_2\eta); \quad \nu, \eta > 0, a_i, b_i > 0 \text{ for } i = 1, 2. \quad (3.3)$$

### 3.1. Posterior analysis

Combining the likelihood function in Equation (2.2) and the joint prior distribution (3.3), the posterior density function of  $(\nu, \eta)$  up to normalizing constant is given by

$$\begin{aligned} \pi^*(\nu, \eta|x) = & K_1^{-1} \left(\frac{2}{\Gamma(\nu)}\right)^D \nu^{\nu D+a_1-1} \eta^{-\nu D+a_2-1} \prod_{i=1}^D x_i^{-(2\nu+1)} e^{-\frac{\nu}{\eta} \sum_{i=1}^D x_i^{-2}} e^{-b_1\nu-b_2\eta} \\ & \prod_{i=1}^D \left[ \frac{\gamma\left(\nu, \frac{\nu}{\eta x_i^2}\right)}{\Gamma(\nu)} \right]^{R_i} \left[ \frac{\gamma\left(\nu, \frac{\nu}{\eta T^2}\right)}{\Gamma(\nu)} \right]^{R^*}, \end{aligned} \quad (3.4)$$

where

$$\begin{aligned} K_1 = & \int_0^\infty \int_0^\infty \left(\frac{2}{\Gamma(\nu)}\right)^D \nu^{\nu D+a_1-1} \eta^{-\nu D+a_2-1} \prod_{i=1}^D x_i^{-(2\nu+1)} e^{-\frac{\nu}{\eta} \sum_{i=1}^D x_i^{-2}} e^{-b_1\nu-b_2\eta} \\ & \prod_{i=1}^D \left[ \frac{\gamma\left(\nu, \frac{\nu}{\eta x_i^2}\right)}{\Gamma(\nu)} \right]^{R_i} \left[ \frac{\gamma\left(\nu, \frac{\nu}{\eta T^2}\right)}{\Gamma(\nu)} \right]^{R^*} d\nu d\eta. \end{aligned}$$

Assume  $v(\nu, \eta)$  denotes the function of  $\nu$  and  $\eta$ . The BEs of function  $v(\nu, \eta)$  under SELF and LLF are given respectively by

$$\begin{aligned} \hat{v}_{SELF}(\nu, \eta) = & K^{-1} \int_0^\infty \int_0^\infty v(\nu, \eta) \left(\frac{2}{\Gamma(\nu)}\right)^D \nu^{\nu D+a_1-1} \eta^{-\nu D+a_2-1} \prod_{i=1}^D x_i^{-(2\nu+1)} e^{-\frac{\nu}{\eta} \sum_{i=1}^D x_i^{-2}} \\ & e^{-b_1\nu-b_2\eta} \prod_{i=1}^D \left[ \frac{\gamma\left(\nu, \frac{\nu}{\eta x_i^2}\right)}{\Gamma(\nu)} \right]^{R_i} \left[ \frac{\gamma\left(\nu, \frac{\nu}{\eta T^2}\right)}{\Gamma(\nu)} \right]^{R^*} d\nu d\eta, \end{aligned} \quad (3.5)$$

and

$$\begin{aligned} \hat{v}_{LLF}(\nu, \eta) = & -\frac{1}{h} \log \left[ K^{-1} \int_0^\infty \int_0^\infty v(\nu, \eta) \left(\frac{2}{\Gamma(\nu)}\right)^D \nu^{\nu D+a_1-1} \eta^{-\nu D+a_2-1} \prod_{i=1}^D x_i^{-(2\nu+1)} \right. \\ & \left. e^{-\frac{\nu}{\eta} \sum_{i=1}^D x_i^{-2}} e^{-b_1\nu-b_2\eta} \prod_{i=1}^D \left[ \frac{\gamma\left(\nu, \frac{\nu}{\eta x_i^2}\right)}{\Gamma(\nu)} \right]^{R_i} \left[ \frac{\gamma\left(\nu, \frac{\nu}{\eta T^2}\right)}{\Gamma(\nu)} \right]^{R^*} d\nu d\eta \right] \end{aligned} \quad (3.6)$$

respectively. In order to compute the BE of  $\nu$  and  $\eta$ , it is necessary to replace  $\nu$  and  $\eta$  in place of the function  $v(\nu, \eta)$  in (3.5) and (3.6). Furthermore, it is seen that the integral involved in Equations (3.5) and (3.6) are very difficult and therefore cannot be solved analytically. Therefore, MCMC approximation techniques are required to derive the approximate BEs. The MCMC is a very popular technique for computing approximate BEs. For additional information on MCMC methods, see *et al.* [25]. Here, we use the Metropolis-Hasting (M-H) algorithm to obtain the BEs of the unknown parameters  $\nu$  and  $\eta$  based on UPHC data, which is described in the following subsection.

### 3.2. Metropolis-Hastings algorithm

The Metropolis-Hastings (M-H) algorithm is a technique for obtaining random samples from complex probability distributions that may be challenging to directly sample from. By constructing a Markov chain- a sequence of interconnected random variables-the algorithm creates a pathway with a stationary distribution matching the desired target distribution. For more details on the M-H algorithm, see Metropolis *et al.* [28] and Hastings [35]. From Equation (3.4), the full conditional posterior pdfs of  $\nu$  and  $\eta$  can be written, respectively, as:

$$\begin{aligned} \pi_1^*(\nu|\eta, x) &\propto \left(\frac{1}{\Gamma(\nu)}\right)^D \nu^{\nu D+a_1-1} \eta^{-\nu D} \prod_{i=1}^D x_i^{-2\nu-1} e^{-\frac{\nu}{\eta} \sum_{i=1}^D x_i^{-2}} e^{-b_1\nu} \\ &\times \prod_{i=1}^D \left[ \frac{\gamma\left(\nu, \frac{\nu}{\eta x_i^2}\right)}{\Gamma(\nu)} \right]^{R_i} \left[ \frac{\gamma\left(\nu, \frac{\nu}{\eta T^2}\right)}{\Gamma(\nu)} \right]^{R^*} \end{aligned} \tag{3.7}$$

and

$$\pi_2^*(\eta|\nu, x) \propto \eta^{-\nu D+a_2-1} e^{-\frac{\nu}{\eta} \sum_{i=1}^D x_i^{-2}} e^{-b_2\nu} \prod_{i=1}^D \left[ \frac{\gamma\left(\nu, \frac{\nu}{\eta x_i^2}\right)}{\Gamma(\nu)} \right]^{R_i} \left[ \frac{\gamma\left(\nu, \frac{\nu}{\eta T^2}\right)}{\Gamma(\nu)} \right]^{R^*}, \tag{3.8}$$

respectively. Note that the conditional posterior pdfs in Equation (3.7) and Equation (3.8) are not in any well-known distribution. So, the M-H algorithm with normal proposal distributional family is used. To compute Bayes estimates and construct associated Bayesian credible intervals of  $\nu$  and  $\eta$ , the following algorithm is considered:

**Step 1:** Start with an initial guess  $\nu^{(0)} = \hat{\nu}$  and  $\eta^{(0)} = \hat{\eta}$ .

**Step 2:** Generate  $\nu^*$  and  $\eta^*$  from the normal proposal distributions  $N(\nu^{(j-1)}, \hat{\sigma}_{\nu\nu})$  and  $N(\eta^{(j-1)}, \hat{\sigma}_{\eta\eta})$ , respectively, for  $j = 1, 2, \dots, N$ .

**Step 3:** Compute the acceptance probabilities for

$$\phi_1(\nu^{(j-1)}, \nu^*) = \min\left(1, \frac{\pi_1^*(\nu^*|\eta^{(j-1)}, x)}{\pi_1^*(\nu^{(j-1)}|\eta^{(j-1)}, x)}\right),$$

and

$$\phi_2(\eta^{(j-1)}, \eta^*) = \min\left(1, \frac{\pi_2^*(\eta^{(j)}|\nu^{(j)}, x)}{\pi_2^*(\eta^{(j-1)}|\nu^{(j)}, x)}\right).$$

**Step 4:** Draw  $u_1$  and  $u_2$  from  $U(0, 1)$ .

**Step 5:** If  $u_1 \leq \phi_1$ , set  $\nu^{(j)} = \nu^*$ ; otherwise, set  $\nu^{(j)} = \nu^{(j-1)}$ . If  $u_2 \leq \phi_2$ , set  $\eta^{(j)} = \eta^*$ ; otherwise, set  $\eta^{(j)} = \eta^{(j-1)}$ .

**Step 6:** Set  $j = j + 1$ .

**Step 7:** Replicate **steps 2-6** up to N times.

Thus, the BEs of  $\nu$  and  $\eta$  under SELF and LLF can be obtained as

$$\hat{\nu}_{SELF} = \frac{\sum_{j=M+1}^N \nu^{(j)}}{N - M}, \quad \hat{\nu}_{LLF} = - \left( \frac{1}{h} \right) \log \left( \frac{\sum_{j=M+1}^N e^{-h\nu^{(j)}}}{N - M} \right), \quad (3.9)$$

and

$$\hat{\eta}_{SELF} = \frac{\sum_{j=M+1}^N \eta^{(j)}}{N - M}, \quad \hat{\eta}_{LLF} = - \left( \frac{1}{h} \right) \log \left( \frac{\sum_{j=M+1}^N e^{-h\eta^{(j)}}}{N - M} \right), \quad (3.10)$$

respectively, where M is the burn-in period of the Markov chain and  $h \neq 0$ .

### 3.3. HPD credible intervals

We follow the technique proposed by Chen and Shao [18] to construct the HPD credible intervals. First, order the simulated MCMC samples of  $\nu^{(j)}$  and  $\eta^{(j)}$  for  $j = 1, \dots, N$  after burn-in as  $(\nu^{(M+1)}, \nu^{(M+2)}, \dots, \nu^{(N)})$  and  $(\eta^{(M+1)}, \eta^{(M+2)}, \dots, \eta^{(N)})$  respectively. Hence,  $100(1 - \psi)\%$  two sided HPD credible intervals for  $\nu$  and  $\eta$  are given by

$$\left[ \nu^{[\frac{(N-M)\psi}{2}]}, \nu^{[(N-M)(1-\frac{\psi}{2})]} \right] \quad \text{and} \quad \left[ \eta^{[\frac{(N-M)\psi}{2}]}, \eta^{[(N-M)(1-\frac{\psi}{2})]} \right]$$

respectively.

### 3.4. Selection of prior-parameter

In Bayesian analysis, the main problem is the elicitation process used to determine the hyperparameter value. The goal of the elicitation process is to capture as accurately as possible the prior uncertainty about the parameters, which serves as a starting point for Bayesian inference. It is essential to conduct elicitation carefully to ensure that the prior distributions are informative and reflect the available knowledge without bias. Many authors investigate this problem in the literature [9, 23, 33]. In this respect, we follow the algorithm of [23] to determine the value of the hyperparameters  $(a_1, b_1)$  and  $(a_2, b_2)$  of  $\nu$  and  $\eta$ , respectively.

The mean and variance of the prior gamma densities given in Equation (3.3) are, respectively, as follows:

$$\frac{1}{B} \sum_{j=1}^B \hat{\nu}^{(j)} = \frac{a_1}{b_1} \quad \text{and} \quad \frac{1}{B-1} \sum_{j=1}^B \left( \hat{\nu}^{(j)} - \frac{1}{B} \sum_{j=1}^B \hat{\nu}^{(j)} \right)^2 = \frac{a_1}{b_1^2}, \quad (3.11)$$

and

$$\frac{1}{B} \sum_{j=1}^B \hat{\eta}^{(j)} = \frac{a_2}{b_2} \quad \text{and} \quad \frac{1}{B-1} \sum_{j=1}^B \left( \hat{\eta}^{(j)} - \frac{1}{B} \sum_{j=1}^B \hat{\eta}^{(j)} \right)^2 = \frac{a_2}{b_2^2}, \quad (3.12)$$

where  $B$  is the total number of replications required to generate  $\hat{\nu}^{(j)}$  and  $\hat{\eta}^{(j)}$  for  $j = 1, 2, \dots, B$ . Using Equation (3.3), the estimated hyperparameter values  $\hat{a}_1$  and  $\hat{b}_1$  of  $a_1$  and  $b_1$  for  $\nu$  can be obtained, respectively, by

$$\hat{a}_1 = \frac{\left( \frac{1}{B} \sum_{j=1}^B \hat{\nu}^{(j)} \right)^2}{\frac{1}{B-1} \sum_{j=1}^B \left( \hat{\nu}^{(j)} - \frac{1}{B} \sum_{j=1}^B \hat{\nu}^{(j)} \right)^2}, \quad (3.13)$$

and

$$\hat{b}_1 = \frac{\frac{1}{B} \sum_{j=1}^B \hat{\nu}^{(j)}}{\frac{1}{B-1} \sum_{j=1}^B \left( \hat{\nu}^{(j)} - B^{-1} \sum_{j=1}^B \hat{\nu}^{(j)} \right)^2}. \tag{3.14}$$

Solving (3.12), the estimated hyperparameters values  $\hat{a}_2$  and  $\hat{b}_2$  of  $a_2$  and  $b_2$  for  $\eta$  can be obtained, respectively, by

$$\hat{a}_2 = \frac{\left( \frac{1}{B} \sum_{j=1}^B \hat{\eta}^{(j)} \right)^2}{\frac{1}{B-1} \sum_{j=1}^B \left( \hat{\eta}^{(j)} - B^{-1} \sum_{j=1}^B \hat{\eta}^{(j)} \right)^2}, \tag{3.15}$$

and

$$\hat{b}_2 = \frac{\frac{1}{B} \sum_{j=1}^B \hat{\eta}^{(j)}}{\frac{1}{B-1} \sum_{j=1}^B \left( \hat{\eta}^{(j)} - B^{-1} \sum_{j=1}^B \hat{\eta}^{(j)} \right)^2}. \tag{3.16}$$

#### 4. Maximum a posteriori estimation

In Bayesian analysis, maximum a posteriori (MAP) estimation refers to estimating the parameters of a statistical model by finding the most probable values given both the observed data and prior knowledge about the parameters. It is a method used to infer the parameters of a model based on Bayes' theorem, which allows us to update our beliefs about the parameters in light of observed data.

If  $\hat{\Theta}_{\text{MAP}}$  represents MAP estimates of the parameters  $\Theta = (\nu, \eta)$  then

$$\begin{aligned} \hat{\Theta}_{\text{MAP}} &= \arg \max_{\Theta} \pi(\Theta | \text{data}) \\ &= \arg \max_{\Theta} \{ \log \pi(\text{data} | \Theta) + \log \pi(\Theta) \}, \end{aligned} \tag{4.1}$$

where  $\pi(\Theta | \text{data})$  is the posterior distribution,  $\pi(\text{data} | \Theta)$  joint distribution of data and  $\pi(\Theta)$  joint prior distribution. Using (3.3) and (3.4), the MAP estimates can be obtained from the following formula:

$$\begin{aligned} \hat{\Theta}_{\text{MAP}} &= \arg \max_{\Theta} \left\{ D \log \left( \frac{1}{\Gamma(\nu)} \right) + (D\nu + a_1 - 1) \log(\nu) + (-D\nu + a_1 - 1) \log(\eta) - (2\nu + 1) \right. \\ &\quad \left. \sum_{i=1}^D \log(x_i) - \frac{\nu}{\eta} \sum_{i=1}^D x_i^{-2} - (b_1\nu + b_2\eta) + \sum_{i=1}^D \log \left[ \frac{\gamma(\nu, \frac{\nu}{\eta x_i^2})}{\Gamma(\nu)} \right] + R^* \log \left[ \frac{\gamma(\nu, \frac{\nu}{\eta T^2})}{\Gamma(\nu)} \right] \right\}. \end{aligned} \tag{4.2}$$

To obtain  $\hat{\alpha}_{\text{MAP}}$  and  $\hat{\beta}_{\text{MAP}}$ , differentiating (4.2) with respect to  $\alpha$  and  $\beta$  respectively, then setting to zero

$$\begin{aligned} &- D \frac{\Gamma(\nu)'}{\Gamma(\nu)} + D \log(\nu) + \frac{(D\nu + a_1 - 1)}{\nu} - D \log(\eta) - 2 \sum_{i=1}^D \log(x_i) - \frac{1}{\eta} \sum_{i=1}^D x_i^{-2} - b_1 \\ &+ \sum_{i=1}^D R_i \frac{\gamma(\nu, \frac{\nu}{\eta x_i^2})'}{\gamma(\nu, \frac{\nu}{\eta x_i^2})} + R^* \frac{\gamma(\nu, \frac{\nu}{\eta T^2})'}{\gamma(\nu, \frac{\nu}{\eta T^2})} - \sum_{i=1}^D R_i \frac{\Gamma(\nu)'}{\Gamma(\nu)} - R^* \frac{\Gamma(\nu)'}{\Gamma(\nu)} = 0 \end{aligned} \tag{4.3}$$

and

$$\frac{-D\nu + a_2 - 1}{\eta} + \frac{\nu}{\eta^2} \sum_{i=1}^D x_i^{-2} - b_2 + \sum_{i=1}^D \frac{\gamma_\eta \left( \nu, \frac{\nu}{\eta x_i^2} \right)'}{\gamma \left( \nu, \frac{\nu}{\eta x_i^2} \right)} + R^* \frac{\gamma_\eta \left( \nu, \frac{\nu}{\eta T^2} \right)'}{\gamma \left( \nu, \frac{\nu}{\eta T^2} \right)} = 0. \tag{4.4}$$

It has been noticed that Equations (4.3) and (4.4) cannot be explicitly solved. To obtain  $\hat{\nu}_{\text{MAP}}$  and  $\hat{\eta}_{\text{MAP}}$ , the nonlinear system of equations given by Equation (4.3) and Equation (4.4) can be solved numerically using the Newton-Rapson iterative method.

### 5. Simulation study

This section conducts a simulation study to examine the behavior of various estimates of  $\nu$  and  $\eta$  under the UPHC scheme. The evaluation of the estimates' performance has been conducted from the following viewpoint:

- **Mean square error (MSE):** Let  $\chi$  and  $\hat{\chi}$  denote the unknown parameters of the associated estimates and  $N$  is the total number of replications. Then, the MSE is defined as follows:

$$\text{MSE}(\hat{\chi}) = \frac{1}{N} \sum_{i=1}^N \left( \hat{\chi}^{(i)} - \chi \right)^2.$$

The smaller value of MSE signifies the superior performance of the estimates.

- **Average bias (AB):** The AB is defined as follows:

$$\text{AB}(\hat{\chi}) = \frac{1}{N} \sum_{i=1}^N \left( \hat{\chi}^{(i)} - \chi \right).$$

A smaller AB value suggests that the experimental data exhibits higher accuracy with the predictive model.

- **Average width (AW):** The AW of the interval estimates at a significance level of  $\psi$  has been assessed. Let  $L_i$  and  $U_i$  be the lower and upper limits of the estimates, then the AW can be written as follows

$$\text{AW}(\hat{\chi}) = \frac{1}{N} \sum_{i=1}^N (U_i - L_i).$$

A shorter length indicates superior performance in the estimation of intervals.

- **Average Coverage probability (ACP):** The probability of containing the actual parameter values within the estimated interval ranges. The average coverage probability (ACP) for the ACI/HPD credible intervals of the unknown parameters are derived using the following formula

$$\text{ACP}(\hat{\chi}) = \frac{1}{N} \sum_{i=1}^N 1_{(U_i;L_i)}(\chi),$$

where  $1(\cdot)$  is the indicator function.

Note that all calculations are executed using R code. To generate  $10^3$  UPHC sample from INK distribution, different combination of  $n, m, k, T_1$ , and  $T_2$  have been taken. The UPHC samples are generated using the algorithm proposed by Kim and Lee [15]. To generate the random sample, the actual values of the parameters are assumed  $\nu = 1.5$  and  $\eta = 2.5$ . Moreover, two different sets of time thresholds  $T_1, T_2$  are taken (1, 2) and (1.5, 2.5). In addition, to this, various sets of sample and effective sample sizes ( $n, m, k$ )

are taken as  $\{(40, 20, 10), (40, 20, 15), (40, 30, 15), (40, 30, 20), (60, 30, 20), (60, 30, 25), (60, 40, 25), (60, 40, 30)\}$ . In this study, three different PCS are adopted:

- **Scheme-A:**  $R_1 = n - m$ ,  $R_i = 0$  for  $i \neq 1$ ,
- **Scheme-B:**  $R_1 = R_m = \frac{n-m}{2}$ ,  $R_i = 0$  for  $i \neq 1, m$ ,
- **Scheme-C:**  $R_m = n - m$ ,  $R_i = 0$  for  $i \neq m$ .

In the Bayesian paradigm, the choice of hyperparameters plays an important role. In this study, the gamma prior distributions are considered as a prior distribution for  $\nu$  and  $\eta$ . For different values of  $n, m, k, T_1, T_2$  and different CS, the hyperparameter values are presented in Table 1.

Using  $10^3$  samples the classical estimates of  $\nu$  and  $\eta$  with their 95% ACIs are calculated. To perform the M-H sampler,  $5 \times 10^3$  MCMC samples are created, and the first  $10^3$  observations are discarded to avoid the effect of the initial guess. So, based on  $4 \times 10^3$  MCMC samples, the expected BE and 95% BCI are calculated. The biases and MSEs of the frequentist and Bayesian approaches of  $\nu$  and  $\eta$  are calculated and provided in Tables 2, 3, 5 and 6, respectively. In addition, the credible intervals 95% ACIs / HPD with average coverage probabilities (CPs) are derived and tabulated in Tables 4 and 7, respectively. All calculations are done using R code via packages "coda" (explored by Plummer *et al.* [24]) and "nleqslv" (proposed by Hasselman and Hasselman [6]). From the numerical result, it is noted that the MLEs and BEs of the unknown parameters produce satisfactory results in terms of average biases and MSE. In addition, for fixed  $n$ , as the failure rate  $m$  increases, the MSE decreases as expected for all estimates. Therefore, increasing the effective sample size may yield more accurate estimation results. In most scenarios, when the threshold time values  $T_1$  and  $T_2$  increase, the AB and MSE of the parameters decrease. Regarding the loss functions, the BEs under LLF ( $h = 0.5$ ) are better than the SELF and MAP for AB and MSE. It is evident from comparing the three censoring schemes ABs and MSEs related to unknown parameters  $\nu$  for scheme A are lower than schemes B and C. Moreover, scheme C has lower ABs and MSEs for the parameter  $\eta$ . The numerical experiment demonstrates that the BEs outperform the two frequentist approaches, namely NR and EM, with regard to MSEs and ABs. Regarding interval estimations, the ACLs of the credible ACI and HPD intervals tend to decrease as the number of failures  $m$  and  $k$  increases. Moreover, the ACLs of the ACI/HPD credible intervals get smaller when the threshold times  $T_1$  and  $T_2$  rise. However, no specific trends were obtained regarding coverage probabilities (ACPs). Tables 4 and 7 show that the ACLs of scheme A are smaller than those of schemes B and C for the parameters  $\nu$ . Moreover, Tables 4 and 7 demonstrate that the ACLs of parameters  $\eta$  are smaller for scheme C than for schemes A and B. In summary, the simulation results show that, in terms of MSEs, ABs, and ACLs, respectively, the performance of the Bayes point and the credible intervals is superior to that of the frequentist approach.

## 6. Optimality

In reliability theory, the optimal choice of a censoring scheme holds significant importance, particularly in scenarios involving progressive censoring. Progressive censoring is a method where data is collected gradually over time. Selecting the best censoring scheme involves considering factors like data type, study goals, resource constraints, and statistical efficiency. This decision directly impacts the accuracy of reliability estimates. By thoughtfully choosing an optimal censoring scheme, researchers can enhance the precision of reliability assessments, ensuring more reliable and trustworthy results in the context of gradually collected data in reliability theory. Recently, the issue of comparing two or more competing censoring plans has gained attention from various authors, for example, [7, 19, 23, 29] among others. The variance optimality criteria are commonly applied to single-parameter distributions, whereas trace and determinant optimality criteria apply

**Table 1.** Hyper-Parameters values based on various censoring schemes.

(n,m)	k	CS	$T_1 = 1, T_2 = 2$				$T_1 = 1.5, T_2 = 2.5$			
			$a_1$	$b_1$	$a_2$	$b_2$	$a_1$	$b_1$	$a_2$	$b_2$
(40,20)	10	A	7.47	4.39	33.08	13.25	9.16	5.58	35.56	14.09
		B	5.77	3.22	46.14	18.35	7.25	4.18	44.93	17.79
		C	5.45	3.00	53.68	21.19	4.98	2.71	56.61	22.35
	15	A	8.61	5.00	36.99	14.63	9.27	5.61	36.10	14.19
		B	7.13	4.15	46.82	18.53	7.27	4.10	47.22	18.58
		C	5.47	3.00	47.50	18.85	5.83	3.16	57.29	22.67
(40,30)	15	A	11.14	6.72	46.99	18.80	14.50	8.89	46.27	18.44
		B	12.20	7.58	57.02	22.78	13.60	8.30	52.00	20.70
		C	11.37	6.91	59.09	23.69	11.98	7.07	58.81	23.26
	20	A	12.41	7.53	47.44	18.89	13.81	8.47	45.64	18.13
		B	13.78	8.47	52.98	21.16	13.74	8.24	51.30	20.44
		C	12.02	7.29	57.09	22.87	14.20	8.60	58.70	23.60
(60,30)	20	A	11.39	6.94	54.44	21.54	15.08	9.33	55.08	21.94
		B	12.20	7.39	67.16	26.61	14.20	8.60	73.50	29.20
		C	9.70	5.64	81.57	32.30	9.87	5.76	81.45	32.31
	25	A	12.66	7.74	55.91	22.26	16.00	10.00	54.20	21.70
		B	11.93	7.15	64.75	25.63	13.57	8.17	70.60	27.97
		C	10.07	5.86	82.00	32.60	9.24	5.39	78.12	30.96
(60,40)	25	A	15.18	9.55	64.91	25.91	19.50	12.20	71.40	28.50
		B	17.01	10.66	75.07	29.94	18.10	11.20	75.70	30.40
		C	15.21	9.32	95.40	38.17	17.90	11.00	88.70	35.30
	30	A	15.49	9.51	67.66	26.86	20.43	12.76	62.22	24.76
		B	17.70	10.85	71.54	28.61	19.18	11.99	78.90	31.47
		C	17.38	10.69	87.30	34.68	16.50	10.18	91.52	36.65

to distributions with multiple parameters. To obtain the optimal PCS, some prevalent criteria for different values of the  $n, m, k$ , and  $T_i, i = 1, 2$ , with censoring scheme  $R_i, i = 1, \dots, m$  are taken. Criteria I and II aim to minimize the trace and determinant of the variance-covariance (V-C) matrix. The comparison of two or more observed V-C matrices is not a trivial task, as criteria I and II are not scale-invariant. However, one can choose the most suitable censoring scheme for a multi-parameter distribution using criteria III, invariant to scale. These criteria are provided in the following Table 8.

**Table 2.** Biases and MSEs (in parentheses) of  $\nu$  for  $(T_1, T_2) = (1, 2)$ .

(n,m)	k	CS	NR	EM	MAP	SELF	LLF	
							h = -0.25	h=0.50
(40,20)	10	A	0.1708 (0.4012)	0.1384 (0.2419)	0.0345 (0.1286)	0.0782 (0.1034)	0.0491 (0.0839)	-0.0162 (0.0721)
		B	0.2986 (0.5909)	0.1675 (0.2878)	0.1136 (0.1382)	0.0896 (0.1208)	0.0606 (0.0916)	0.0588 (0.1018)
		C	0.3329 (0.6141)	0.1605 (0.3585)	0.1184 (0.1378)	0.1279 (0.1383)	0.0799 (0.1110)	0.0594 (0.0993)
	15	A	0.1795 (0.3574)	0.1388 (0.2408)	0.0579 (0.0757)	0.1027 (0.0984)	0.0705 (0.0715)	0.0066 (0.0576)
		B	0.2724 (0.5023)	0.1620 (0.2482)	0.0836 (0.1050)	0.1875 (0.1482)	0.1070 (0.1047)	0.0367 (0.0799)
		C	0.2839 (0.6048)	0.1440 (0.3368)	0.0907 (0.1334)	0.2312 (0.2084)	0.1256 (0.1368)	0.0369 (0.0989)
(40,30)	15	A	0.1281 (0.2703)	0.1373 (0.2361)	0.0404 (0.0611)	0.0997 (0.0723)	0.0463 (0.0579)	-0.0023 (0.0504)
		B	0.1224 (0.2335)	0.1666 (0.2237)	0.0270 (0.0483)	0.0781 (0.0564)	0.0313 (0.0465)	-0.0116 (0.0416)
		C	0.1541 (0.2580)	0.1646 (0.2204)	0.0509 (0.0597)	0.1069 (0.0726)	0.0580 (0.0579)	0.0131 (0.0492)
	20	A	0.1332 (0.2431)	0.1480 (0.1858)	0.0439 (0.1277)	0.0996 (0.0627)	0.0494 (0.0499)	0.0035 (0.0430)
		B	0.1448 (0.2326)	0.1287 (0.2096)	0.0491 (0.0473)	0.0979 (0.0570)	0.0527 (0.0458)	0.0110 (0.0394)
		C	0.1150 (0.2307)	0.1124 (0.1998)	0.0336 (0.0564)	0.0886 (0.0674)	0.0417 (0.0551)	-0.0013 (0.0482)
(60,30)	20	A	0.1162 (0.2048)	0.1297 (0.1638)	0.0364 (0.0512)	0.0977 (0.0621)	0.0478 (0.0496)	0.0021 (0.0430)
		B	0.1525 (0.2237)	0.1393 (0.1882)	0.0614 (0.0539)	0.1270 (0.0711)	0.0795 (0.0552)	0.0357 (0.0451)
		C	0.2185 (0.3284)	0.1209 (0.2221)	0.0932 (0.0717)	0.1866 (0.1093)	0.1238 (0.0793)	0.0674 (0.0602)
	25	A	0.1220 (0.2002)	0.1186 (0.1623)	0.0550 (0.0507)	0.1090 (0.0620)	0.0635 (0.0489)	0.0215 (0.0418)
		B	0.1415 (0.2177)	0.1350 (0.1802)	0.0534 (0.0419)	0.1121 (0.0619)	0.0634 (0.0454)	0.0334 (0.0409)
		C	0.2180 (0.3001)	0.1199 (0.2201)	0.0834 (0.0611)	0.0668 (0.0899)	0.0742 (0.0652)	0.0591 (0.0525)
(60,40)	25	A	0.0813 (0.1531)	0.0905 (0.1298)	0.0156 (0.0368)	0.0591 (0.0414)	0.0217 (0.0354)	-0.0132 (0.0325)
		B	0.1021 (0.1609)	0.1306 (0.1504)	0.0337 (0.0388)	0.0730 (0.0454)	0.0398 (0.0388)	0.0086 (0.0348)
		C	0.1339 (0.1982)	0.1161 (0.2082)	0.0532 (0.0455)	0.0977 (0.0552)	0.0610 (0.0452)	0.0265 (0.0386)
	30	A	0.0808 (0.1484)	0.0805 (0.1225)	0.0151 (0.0311)	0.0580 (0.0401)	0.0209 (0.0339)	-0.0102 (0.0319)
		B	0.1001 (0.1580)	0.0999 (0.1382)	0.0321 (0.0374)	0.0322 (0.0359)	0.0327 (0.0359)	0.0302 (0.0342)
		C	0.1261 (0.1751)	0.0997 (0.1582)	0.0488 (0.0434)	0.0772 (0.0532)	0.0532 (0.0442)	0.0202 (0.0366)

**Table 3.** Biases and MSEs (in parenthesis) of  $\eta$  for  $(T_1, T_2) = (1, 2)$ .

(n,m)	k	CS	NR	EM	MAP	SELF	LLF	
							h = -0.25	h=0.50
(40,20)	10	A	0.0630 (0.1829)	0.0337 (0.1637)	-0.0169 (0.0441)	0.0561 (0.0475)	0.0565 (0.0476)	-0.0257 (0.0412)
		B	0.0078 (0.1395)	-0.0177 (0.1289)	-0.0267 (0.0759)	0.0652 (0.0711)	0.0654 (0.0712)	0.0158 (0.0567)
		C	0.0202 (0.1230)	-0.0125 (0.1077)	-0.0120 (0.0796)	0.0303 (0.0854)	0.0112 (0.0763)	0.0424 (0.0680)
	15	A	0.0370 (0.1823)	0.0230 (0.1601)	-0.0155 (0.0437)	0.0545 (0.0463)	0.0150 (0.0417)	-0.0225 (0.0403)
		B	0.0198 (0.1315)	-0.0151 (0.1214)	-0.0325 (0.0736)	0.0173 (0.0633)	0.0122 (0.0556)	0.1079 (0.0494)
		C	0.0196 (0.1229)	-0.0177 (0.1073)	-0.0186 (0.0719)	0.0392 (0.0835)	0.0188 (0.0733)	0.0587 (0.0641)
(40,30)	15	A	0.0194 (0.1322)	0.0199 (0.1159)	-0.0241 (0.0337)	0.0222 (0.0341)	-0.0088 (0.0326)	-0.0387 (0.0330)
		B	0.0022 (0.1216)	-0.0115 (0.1087)	-0.0266 (0.0293)	0.0169 (0.0318)	-0.0100 (0.0311)	-0.0359 (0.0318)
		C	-0.0077 (0.1031)	-0.0110 (0.1004)	-0.0337 (0.0673)	0.0658 (0.0515)	0.0445 (0.0596)	0.0239 (0.0586)
	20	A	0.0089 (0.1368)	0.0207 (0.0891)	-0.0235 (0.0352)	0.02315 (0.0355)	-0.0078 (0.0339)	-0.0374 (0.0342)
		B	0.0143 (0.1236)	0.0194 (0.1002)	-0.0210 (0.0317)	0.0257 (0.0356)	-0.0016 (0.0344)	-0.0291 (0.0346)
		C	0.0327 (0.0793)	0.00877 (0.0673)	0.0051 (0.0480)	0.0237 (0.0762)	0.0225 (0.0704)	0.0214 (0.0629)
(60,30)	20	A	0.0108 (0.1227)	-0.0151 (0.0728)	-0.0124 (0.0294)	0.0391 (0.0308)	0.0118 (0.0285)	-0.0145 (0.0278)
		B	0.0163 (0.0829)	-0.0210 (0.0717)	-0.0068 (0.0221)	0.1800 (0.0576)	0.1639 (0.0519)	0.1481 (0.0468)
		C	0.0144 (0.0522)	-0.0113 (0.0451)	-0.0147 (0.0416)	-0.0031 (0.0416)	-0.0029 (0.0416)	-0.0041 (0.0416)
	25	A	0.0250 (0.1222)	-0.0177 (0.0688)	-0.0154 (0.0284)	0.0328 (0.0292)	0.0063 (0.0274)	-0.0193 (0.0269)
		B	0.0250 (0.1222)	-0.0179 (0.0628)	-0.0154 (0.0284)	0.0328 (0.0292)	0.0063 (0.0274)	-0.0193 (0.0269)
		C	0.0206 (0.0521)	0.0158 (0.0408)	-0.0109 (0.0404)	0.0007 (0.0405)	0.0008 (0.0405)	-0.0004 (0.0405)
(60,40)	25	A	0.0017 (0.0899)	-0.0035 (0.0473)	-0.0213 (0.0225)	0.0166 (0.0224)	-0.0061 (0.0216)	-0.0283 (0.0209)
		B	0.0092 (0.0822)	0.0045 (0.0599)	-0.0124 (0.0311)	0.0474 (0.0316)	0.0291 (0.0304)	0.0113 (0.0298)
		C	0.0121 (0.0690)	-0.0070 (0.0669)	-0.0189 (0.0365)	0.1390 (0.0377)	0.1280 (0.0347)	0.0172 (0.0320)
	30	A	0.0056 (0.0618)	-0.0039 (0.0321)	-0.0171 (0.0212)	-0.0066 (0.0212)	-0.0065 (0.0212)	-0.0078 (0.0211)
		B	-0.0094 (0.0504)	-0.010 (0.0358)	-0.0201 (0.0238)	-0.0093 (0.0229)	-0.0092 (0.0229)	-0.0104 (0.0227)
		C	0.0109 (0.0456)	0.0122 (0.0400)	-0.0139 (0.0280)	-0.0039 (0.0271)	-0.0042 (0.0272)	-0.0039 (0.0261)

**Table 4.** ACI, HDI and CP of  $\nu$  and  $\eta$  for  $(T_1, T_2) = (1, 2)$ .

(n,m)	k	CS	$\nu$				$\eta$			
			ACI	CP	HDI	CP	ACI	CP	HDI	CP
(40,20)	10	A	2.1915	0.9570	1.5341	0.9890	1.6754	0.9600	1.1481	0.9900
		B	2.2587	0.9570	1.6691	0.9750	1.3709	0.9140	0.9041	0.9360
		C	2.5292	0.9620	1.8153	0.9860	1.2632	0.9180	0.7836	0.8270
	15	A	2.1651	0.9590	1.4833	0.9910	1.6392	0.9330	1.1173	0.9920
		B	2.2224	0.9480	1.5632	0.9850	1.3641	0.9300	0.9038	0.9410
		C	2.4590	0.9580	1.7882	0.9830	1.2795	0.9210	0.8070	0.8150
(40,30)	15	A	1.8225	0.9520	1.2753	0.9960	1.4159	0.9410	0.9874	0.9910
		B	1.7146	0.9610	1.1962	0.9940	1.3207	0.9270	0.9179	0.9820
		C	1.7093	0.9470	1.2222	0.9900	1.2415	0.9310	0.8249	0.9630
	20	A	1.8153	0.9550	1.2390	0.9920	1.4026	0.9340	0.9840	0.9900
		B	1.7315	0.9530	1.1758	0.9930	1.3192	0.9320	0.9265	0.9790
		C	1.6692	0.9450	1.1964	0.9920	1.2635	0.9300	0.8407	0.9490
(60,30)	20	A	1.7479	0.9640	1.2354	0.9950	1.3554	0.9350	0.9271	0.9930
		B	1.6958	0.9660	1.2051	0.9930	1.1524	0.9460	0.7245	0.8940
		C	1.9309	0.9700	1.3906	0.9910	1.0494	0.9330	0.6178	0.8980
	25	A	1.6893	0.9620	1.1769	0.9900	1.3384	0.9340	0.9152	0.9940
		B	1.6904	0.9480	1.1879	0.9990	1.1221	0.9490	0.7180	0.9120
		C	1.8775	0.9750	1.0905	0.9910	1.0431	0.9390	0.6105	0.9180
(60,40)	25	A	1.4513	0.9460	1.1030	0.9920	1.1526	0.9470	0.8651	0.9660
		B	1.4200	0.9500	1.0111	0.9940	1.1062	0.9370	0.7632	0.9530
		C	1.4765	0.9540	1.0626	0.9800	1.0205	0.9350	0.5988	0.9040
	30	A	1.4493	0.9600	1.1004	0.9990	1.0931	0.9390	0.8587	0.9710
		B	1.4115	0.9450	1.0067	0.9970	1.0462	0.9390	0.7534	0.9630
		C	1.4545	0.9610	1.0081	0.9950	1.0009	0.9500	0.5899	0.9510

**Table 5.** Biases and MSEs (in parenthesis) of  $\nu$  for  $(T_1, T_2) = (1.5, 2.5)$ .

(n,m)	k	CS	NR	EM	MAP	SELF	LLF	
							h = -0.25	h=0.50
(40,20)	10	A	0.1992 (0.3914)	0.1456 (0.2416)	0.0276 (0.0656)	0.0978 (0.0801)	0.0984 (0.0803)	-0.0156 (0.0544)
		B	0.2734 (0.4990)	0.1576 (0.2858)	0.0901 (0.1021)	0.1934 (0.1477)	0.1943 (0.1483)	0.0432 (0.0782)
		C	0.3182 (0.5079)	0.1602 (0.3495)	0.0442 (0.1074)	0.0813 (0.1089)	0.0790 (0.1088)	-0.0063 (0.0828)
	15	A	0.2052 (0.3449)	0.1442 (0.2410)	0.0086 (0.0562)	0.0760 (0.0660)	0.0207 (0.0533)	-0.0293 (0.0478)
		B	0.2505 (0.4453)	0.1542 (0.2804)	0.0440 (0.0684)	0.1342 (0.0950)	0.0640 (0.0686)	0.0018 (0.0550)
		C	0.3014 (0.4519)	0.1568 (0.3384)	-0.0195 (0.0741)	0.1204 (0.3841)	0.0251 (0.0751)	-0.0445 (0.0638)
(40,30)	15	A	0.1221 (0.1981)	0.1245 (0.2311)	0.0453 (0.0456)	0.0886 (0.0532)	0.0484 (0.0436)	0.0109 (0.0379)
		B	0.1401 (0.2603)	0.1171 (0.2188)	0.0514 (0.0269)	0.1089 (0.0400)	0.1093 (0.0404)	0.1047 (0.0382)
		C	0.1476 (0.2252)	0.1641 (0.2171)	0.1898 (0.0987)	0.2411 (0.1251)	0.1895 (0.0952)	0.1421 (0.0732)
	20	A	0.0947 (0.1784)	0.1355 (0.1654)	0.0307 (0.0444)	0.0753 (0.0507)	0.0348 (0.0423)	-0.0029 (0.0376)
		B	0.1566 (0.2372)	0.1808 (0.1790)	0.0707 (0.0544)	0.1174 (0.0660)	0.0751 (0.0525)	0.0358 (0.0436)
		C	0.1448 (0.2161)	0.1225 (0.1901)	0.0546 (0.0460)	0.1043 (0.0571)	0.0613 (0.0452)	0.0215 (0.0379)
(60,30)	20	A	0.1192 (0.1734)	0.1394 (0.1577)	0.0419 (0.0415)	0.0883 (0.0499)	0.0501 (0.0411)	0.0144 (0.0358)
		B	0.1371 (0.2296)	0.1309 (0.1796)	0.0678 (0.0511)	0.1274 (0.0656)	0.0832 (0.0520)	0.0423 (0.0434)
		C	0.1935 (0.3086)	0.1190 (0.2210)	0.0798 (0.0686)	0.1691 (0.1022)	0.1080 (0.0752)	0.0529 (0.0583)
	25	A	0.1059 (0.1698)	0.1132 (0.1524)	0.2219 (0.1057)	0.2724 (0.1336)	0.2257 (0.1047)	0.1823 (0.0823)
		B	0.1534 (0.2566)	0.1380 (0.1800)	-0.0049 (0.0141)	0.0369 (0.0169)	0.0372 (0.0168)	0.0342 (0.0162)
		C	0.1731 (0.3040)	0.1281 (0.2150)	-0.0024 (0.0445)	0.0397 (0.0468)	0.0400 (0.0469)	0.0369 (0.0465)
(60,40)	25	A	0.0992 (0.1291)	0.0871 (0.1154)	0.0409 (0.0314)	0.0737 (0.0363)	0.0444 (0.0308)	0.0166 (0.0273)
		B	0.0972 (0.1387)	0.0992 (0.1280)	0.0393 (0.0344)	0.0776 (0.0411)	0.0467 (0.0345)	0.0175 (0.0302)
		C	0.1153 (0.1631)	0.1176 (0.2078)	0.0480 (0.0365)	0.0887 (0.0446)	0.0551 (0.0367)	0.0234 (0.0316)
	30	A	0.0748 (0.1285)	0.0861 (0.1101)	0.0307 (0.0312)	0.0625 (0.0352)	0.0341 (0.0304)	0.0071 (0.0271)
		B	0.1130 (0.1311)	0.1051 (0.0923)	0.0409 (0.0340)	0.0773 (0.0401)	0.0472 (0.0337)	0.0186 (0.0295)
		C	0.1239 (0.1608)	0.0915 (0.1362)	0.0671 (0.0349)	0.1048 (0.0437)	0.0711 (0.0357)	0.0394 (0.0315)

**Table 6.** Biases and MSEs (in parenthesis) of  $\eta$  for  $(T_1, T_2) = (1.5, 2.5)$ .

(n,m)	k	CS	NR	EM	MAP	SELF	LLF	
							h = -0.25	h=0.50
(40,20)	10	A	0.0122 (0.1679)	-0.0487 (0.1621)	-0.0301 (0.0425)	0.0412 (0.0436)	0.0416 (0.0436)	-0.0374 (0.0399)
		B	0.0386 (0.1396)	0.0264 (0.1216)	-0.0084 (0.0761)	0.2015 (0.0749)	0.2018 (0.0750)	0.1516 (0.0557)
		C	-0.0268 (0.1177)	-0.0438 (0.0985)	-0.0292 (0.0789)	0.2093 (0.0727)	0.1905 (0.0645)	0.1721 (0.0572)
	15	A	0.0607 (0.1641)	0.0164 (0.1542)	-0.0500 (0.0405)	0.0176 (0.0382)	-0.0203 (0.0367)	-0.0566 (0.0381)
		B	0.0318 (0.1338)	0.0026 (0.1217)	0.0207 (0.0758)	0.2296 (0.0864)	0.2039 (0.0744)	0.1690 (0.0541)
		C	0.0218 (0.1126)	-0.0106 (0.0955)	-0.0844 (0.0598)	0.1271 (0.0586)	0.1091 (0.0548)	0.0916 (0.0499)
(40,30)	15	A	0.0049 (0.1426)	-0.0034 (0.1141)	-0.0279 (0.0381)	0.0189 (0.0380)	-0.0123 (0.0366)	-0.0422 (0.0372)
		B	-0.0049 (0.0746)	-0.0057 (0.0990)	-0.0060 (0.0496)	0.0103 (0.0470)	0.0104 (0.0462)	0.0087 (0.0469)
		C	-0.0028 (0.1119)	-0.0085 (0.0998)	0.0074 (0.0618)	0.1602 (0.0577)	0.1422 (0.0518)	0.1247 (0.0466)
	20	A	0.0106 (0.1364)	0.0027 (0.0819)	-0.0208 (0.0375)	0.0269 (0.0370)	-0.0050 (0.0352)	-0.0354 (0.0343)
		B	-0.0053 (0.1119)	-0.0116 (0.0915)	-0.0281 (0.0418)	0.0821 (0.0396)	0.0582 (0.0358)	0.0353 (0.0332)
		C	0.01532 (0.1076)	0.0097 (0.1056)	-0.0259 (0.0569)	0.1202 (0.0518)	0.1019 (0.0472)	0.0839 (0.0434)
(60,30)	20	A	0.0323 (0.1170)	0.0061 (0.0613)	-0.0106 (0.0346)	0.0380 (0.0289)	0.0113 (0.0267)	-0.0145 (0.0260)
		B	0.0057 (0.0877)	-0.0104 (0.0736)	-0.0139 (0.0413)	0.1703 (0.0391)	0.1555 (0.0340)	0.14098 (0.0334)
		C	0.0190 (0.0796)	-0.0111 (0.0682)	-0.0086 (0.0482)	0.0224 (0.0402)	0.0212 (0.0387)	0.0200 (0.0385)
	25	A	0.0339 (0.0775)	0.0060 (0.0609)	-0.0107 (0.0325)	0.00285 (0.0257)	0.0029 (0.0217)	-0.0024 (0.0216)
		B	0.0138 (0.0542)	0.0030 (0.0521)	-0.0127 (0.0391)	-0.0017 (0.0280)	-0.0016 (0.0270)	-0.0029 (0.0263)
		C	0.0206 (0.0475)	0.0058 (0.0408)	-0.0109 (0.0395)	0.0007 (0.0304)	0.0008 (0.0291)	-0.0004 (0.0255)
(60,40)	25	A	0.0003 (0.0714)	-0.0071 (0.0491)	-0.0208 (0.0318)	0.0138 (0.0215)	-0.0077 (0.0209)	-0.0283 (0.0203)
		B	0.0859 (0.0493)	0.0637 (0.0365)	0.0225 (0.0366)	0.0329 (0.0235)	0.0297 (0.0235)	0.0270 (0.0241)
		C	0.0105 (0.0694)	0.0036 (0.0666)	-0.0072 (0.0278)	0.1635 (0.0261)	0.1522 (0.0263)	0.1411 (0.0269)
	30	A	0.0094 (0.0887)	0.0010 (0.0476)	-0.0138 (0.0307)	0.0235 (0.0228)	0.0005 (0.0207)	-0.0218 (0.0201)
		B	0.0122 (0.0794)	0.0039 (0.0362)	-0.0118 (0.0305)	0.1150 (0.0231)	0.1005 (0.0223)	0.0864 (0.0219)
		C	0.0044 (0.0682)	0.0002 (0.0658)	-0.0139 (0.0274)	-0.0039 (0.0259)	-0.0038 (0.0254)	-0.0049 (0.0251)

**Table 7.** ACI, HDI and CP of  $\nu$  and  $\eta$  for  $(T_1, T_2) = (1.5, 2.5)$ .

(n,m)	k	CS	$\nu$				$\eta$			
			ACI	CP	HDI	CP	ACI	CP	HDI	CP
(40,20)	10	A	1.9108	0.9620	1.3479	0.9940	1.6170	0.9390	1.1270	0.9930
		B	2.2148	0.9660	1.5592	0.9950	1.3942	0.9270	0.9123	0.9260
		C	2.3012	0.9600	1.7732	0.9930	1.2781	0.9200	0.7743	0.8900
	15	A	1.8673	0.9500	1.2942	0.9950	1.6208	0.9420	1.0925	0.9890
		B	2.1843	0.9740	1.4615	0.9950	1.3922	0.9220	0.9070	0.9000
		C	2.2371	0.9520	1.6211	0.9860	1.2654	0.9400	0.7486	0.9730
(40,30)	15	A	1.5904	0.9150	1.1211	0.9920	1.5218	0.9300	1.0065	0.9920
		B	1.5986	0.9550	1.1305	0.9870	1.3069	0.9410	0.8868	0.9780
		C	1.6645	0.9610	1.2562	0.9730	1.2402	0.9170	0.7309	0.9200
	20	A	1.5517	0.9540	1.1124	0.9900	1.4056	0.9380	1.0014	0.9900
		B	1.6009	0.9520	1.1363	0.9910	1.2967	0.9250	0.8810	0.9800
		C	1.6616	0.9670	1.1453	0.9980	1.2501	0.9330	0.7757	0.9580
(60,30)	20	A	1.5354	0.9580	1.0816	0.9910	1.3485	0.9420	0.9165	0.9950
		B	1.7093	0.9610	1.1632	0.9940	1.1446	0.9400	0.6968	0.9090
		C	1.9021	0.9670	1.3703	0.9900	1.0463	0.9280	0.6190	0.9350
	25	A	1.5330	0.9560	1.0201	0.9930	1.3298	0.9440	0.9121	0.9960
		B	1.6833	0.9620	1.1361	0.9930	1.1201	0.9420	0.6812	0.9210
		C	1.8256	0.9690	1.3280	0.9910	1.0190	0.9290	0.6099	0.9420
(60,40)	25	A	1.3400	0.9580	0.9478	0.9980	1.1943	0.9370	0.8301	0.9920
		B	1.3520	0.9620	0.9740	0.9910	1.1029	0.9280	0.6973	0.9530
		C	1.4568	0.9540	1.0172	0.9900	1.0283	0.9350	0.6074	0.8650
	30	A	1.3209	0.9540	0.9330	0.9890	1.1901	0.9520	0.8527	0.9970
		B	1.3466	0.9510	0.9612	0.9910	1.1001	0.9420	0.6923	0.9590
		C	1.4553	0.9620	1.0164	0.9910	1.0246	0.9410	0.6051	0.8990

**Table 8.** Various optimality criterion.

Criterion	Goal
I	Min. $trace(I^{-1}(\hat{\nu}, \hat{\eta}))$
II	Min. $det(I^{-1}(\hat{\nu}, \hat{\eta}))$
III	Max. $trace(I(\hat{\nu}, \hat{\eta}))$

## 7. Application

In this section, we analyze two data sets that represent the fracture toughness of silicon nitrate ( $Si_3N_4$ ) and active repair times (in hours) for an airborne communication transceiver.

### 7.1. Application I

Dataset I represents the fracture toughness of silicon nitrate ( $Si_3N_4$ ). Fracture toughness data are crucial to understanding the mechanical behavior of materials such as silicon nitride ( $Si_3N_4$ ). Silicon nitride is renowned for its excellent mechanical properties, including high strength and toughness. Measurements of fracture toughness reveal the resistance of a material to crack propagation, which is crucial for creating strong structural parts and designing robust structural components in demanding applications such as the aerospace and automotive industries. Accurate fracture toughness data enable engineers and researchers to assess the reliability and performance of the material under varying loading conditions, facilitating the development of advanced materials based on  $Si_3N_4$  tailored for specific industrial needs. Panahi [11] first analyzed the complete fracture toughness data set for silicon nitride and fitted it to the Burr-III distribution. Later, Dutta and Kayal [34] reexamined the same data and applied the Burr-III distribution again.

First, we fit the INK distribution to complete fracture toughness data along with five various lifetime models as its competitors, namely: Burr III (B-III), inverse Weibull (IW), inverse Gompertz (IG), inverse Maxwell (IM), and inverse Rayleigh (IR) distribution. To verify the validity of the INK distribution along with other competent distributions, the Kolmogorov-Smirnov distance (K-S) along with the associated p-value, the negative log-likelihood criterion (NLC), the Akaike information criterion (AIC), the Bayesian information criterion (BIC), the Hannan-Quinn information criterion (HQIC), and the Akaike information criterion with correction (AICC) are calculated and presented in Table 9. In addition, the MLEs with their standard errors (SE) of the unknown parameters are calculated and tabulated in the same Table 9. It shows that the INK distribution is the best model among all competitive fit distributions for fitting fracture toughness data sets because its p-value is the highest and its goodness-of-fit values are the smallest. For a pictorial representation, the histogram and density plots of the INK, B-III, IW, IG, IM, and IR distributions of the data set are shown in Figure 4 and validate our findings. Furthermore, the empirical CDF (ECDF) and CDF of the data set are plotted in Figure 5. These plots confirmed that the INK distribution approximates the general pattern of the histograms of the fracture toughness datasets. Therefore, the visual representation validates the numerical results. Moreover, to show the existence and uniqueness of MLE for the real dataset, the contour plot for  $\nu$  and  $\eta$  is plotted and shown in Figure 3. It shows that MLEs may exist uniquely.

Using complete fracture toughness data sets, three different artificial UPHC samples with  $m = 24, 28,$  and  $30$  and various choices of  $\mathbf{R}$  and  $T_1$  and  $T_2$ . Table 10 provides the created samples and the associated censoring scheme. In short, the scheme  $R =$

$(2, 0, 0, 0, 2)$  is assumed to be  $R = (2, 0^*3, 2)$ . Utilizing the generated sample presented in Table 10, the point estimates of unknown parameters under frequentist and BEs are calculated and provided in Table 11. In addition, the 95% ACIs and HPD credible intervals of the unknown parameters with their average lengths (ALs) are obtained and tabulated in Table 12. While computing BEs, since no prior information is available for the parameters  $\nu$  and  $\eta$  therefore non-informative priors, i.e.  $a_1 = a_2 = 0$  and  $b_1 = b_2 = 0$  are considered. However, to perform the calculation, we consider all  $a_i$  and  $b_i = 0.001$  for  $i = 1, 2$ .

Applying the MCMC technique described in Section 3.2, the first  $10^4$  iterations of the  $5 \times 10^4$  MCMC samples have been eliminated to remove the impacts from the starting values. The starting values of  $\nu_0$  and  $\eta_0$  are assumed to be their MLEs to run the MCMC sampler. Furthermore, to check the convergence of the MCMC sample, the trace plots based on the  $5 \times 10^4$  MCMC chain values of  $\nu$  and  $\eta$  are plotted and shown in Figure 6. In each trace plot, the solid line (—) represents the mean sample, and the dotted line (---) denotes the two limits of 95% HPD credible intervals. From these plots, it is seen that the chain is well mixed and converges quite well. Furthermore, based on the  $4 \times 10^4$  MCMC samples, the histogram and kernel density plots of  $\nu$  and  $\eta$  are plotted and depicted in Figure 7. The posterior sample generated from  $\nu$  and  $\eta$  is observed to be fairly symmetric, leading to a positive indication of the convergence of the MCMC sample. In addition, the autocorrelation plots based on the MCMC samples  $4 \times 10^4$  are plotted and shown in Figure 8. The autocorrelation is rapidly decreasing, indicating that the chain is mixing well and that the samples are becoming less dependent on their predecessors, which supports our convergence of MCMC samples.

To clarify the concept of an optimal censoring plan, the different criteria presented in Table 8 are considered based on three created samples. The available data yield more accurate estimations of survival probabilities by optimizing the trace. The values of all three criteria based on the created samples are calculated and provided in Table 17. Of the aforementioned criteria, it is evident that the best censoring scheme has the lowest value of criteria I and II and the highest value of criterion III. Table 14 indicates that Scheme C with censoring scheme  $R = (0^*29, 0^*23)$  is optimal for criteria I and II. In Criteria III, scheme B with censoring scheme  $R = (4^*1, 0^*26, 4^*1)$  is optimal.

## Application II

Dataset II represents active repair times (in hours) for an airborne communication transceiver ( $n=40$ ), originally proposed by Jorgensen [14]. To assess the suitability of the INK distribution for this dataset, we computed the KS test statistic and the corresponding p-value. The distance from KS was found to be 0.1033, with a p-value of 0.7867. These results indicate that the INK distribution provides an adequate fit to dataset II.

Using the complete data set II, three different artificial UPHC samples with  $m = 20, 24$  and 30 are created and various choices of  $\mathbf{R}$  and  $T_1$  and  $T_2$ . Table 14 provides the created samples and the associated censoring scheme. Utilizing the generated sample presented in Table 14, the point estimates of unknown parameters under frequentist and BEs are calculated and provided in Table 15. In addition, the 95% ACIs and HPD credible intervals of the unknown parameters with their average lengths (ALs) are obtained and tabulated in Table 16. While computing BEs, since no prior information is available for the parameters  $\nu$  and  $\eta$  therefore non-informative priors, i.e.  $a_1 = a_2 = 0$  and  $b_1 = b_2 = 0$  are considered. However, to perform the calculation, we consider all  $a_i$  and  $b_i = 0.001$  for  $i = 1, 2$ .

We evaluated three sample data sets and evaluated them using the criteria listed in Table 8 to better understand the idea of an optimal censoring plan. The results for all three criteria based on these samples are shown in Table 17. Among the criteria, the best censoring scheme is the one with the lowest values for criteria I and II and the highest value

for criterion III. According to Table 17, Scheme C with censoring plan  $R = (029, 101)$  is found to be optimal for all three criteria.

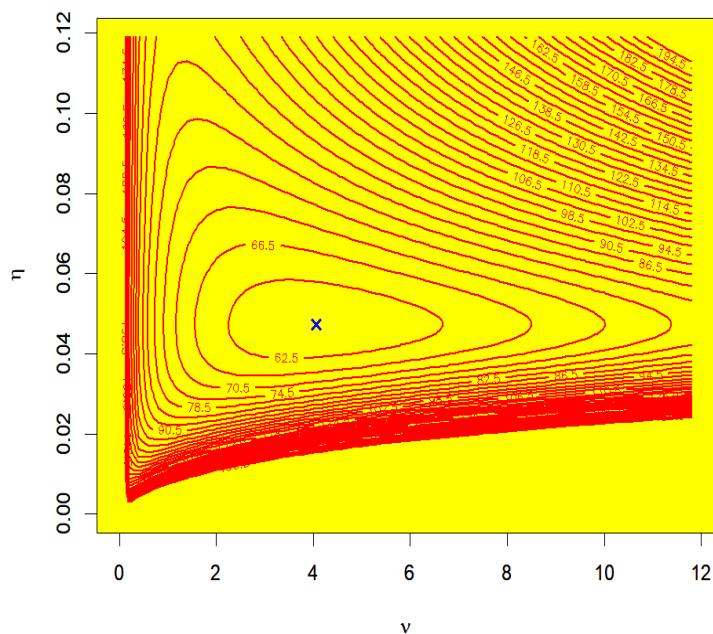


Figure 3. Contour plot of log-LF for different choices of  $\nu$  and  $\eta$  for dataset I.

Table 9. Goodness of fit test and MLEs (with SEs) for dataset I.

Model	$\hat{\nu}$	$\hat{\eta}$	-2NLC	AIC	BIC	HQIC	AICC	K-S	p-value
INK	<b>4.052(0.918)</b>	<b>0.047(0.004)</b>	<b>119.299</b>	<b>123.299</b>	<b>127.585</b>	<b>124.985</b>	<b>123.499</b>	<b>0.075</b>	<b>0.988</b>
B-III	215.869(115.680)	3.665(0.387)	123.754	127.754	130.921	128.859	128.117	0.111	0.771
IW	113.984(52.236)	3.226(0.327)	126.188	130.188	133.355	131.293	130.552	0.122	0.653
IG	0.432(0.194)	15.071(1.981)	132.830	136.830	139.997	137.935	137.194	0.145	0.435
IM	-	0.032(0.004)	133.940	135.940	137.523	136.492	136.057	0.197	0.121
IR	-	21.136(3.523)	145.802	147.802	149.385	148.355	147.920	0.279	0.007

**Table 10.** Three artificial UPHC schemes for dataset I

(n,m,k)	Scheme	UPHC sample	(T <sub>1</sub> , T <sub>2</sub> )	D	R*	T*
(36,24,16)	R = (12*1, 0*23)	2.70, 4.53, 4.60, 4.61, 4.70, 4.70, 4.90, 4.96, 4.98, 5.02, 5.22, 5.25, 5.36, 5.40, 5.50, 6.00	(5,7)	16	8	6
(36,28,20)	R = (4*1, 0*26, 4*1)	2.70, 3.96, 4.00, 4.00, 4.10, 4.26, 4.30, 4.30, 4.50, 4.53, 4.60, 4.61, 4.70, 4.70, 4.90, 4.96, 4.98, 5.02, 5.22, 5.25,	(5,6)	20	12	5.25
(36,30,24)	R = (0*29, 6*1)	2.70, 3.12, 3.20, 3.70, 3.80, 3.96, 4.00, 4.00, 4.10, 4.26, 4.30, 4.30, 4.50, 4.53, 4.60, 4.61, 4.70, 4.70, 4.90, 4.96, 4.98	(4,5)	21	15	5

**Table 11.** Point estimates  $\nu$  and  $\eta$  (with their SEs) based on dataset I.

(n,m)	k	CS	Parameters	NR	EM	MAP	SELF	LLF	
								p = -0.25	p = 0.50
(36,24)	16	A	$\nu$	3.4622	3.4614	2.9666	3.2738	3.3109	2.9525
			$\eta$	0.0368	0.0368	0.0360	0.0371	0.0371	0.0370
(36,28)	20	B	$\nu$	4.9763	4.9751	3.9680	4.6969	5.0498	4.1551
			$\eta$	0.0430	0.0431	0.0422	0.0431	0.0431	0.0432
(36,30)	24	C	$\nu$	3.8365	3.8355	3.3725	3.6262	3.8314	3.2915
			$\eta$	0.0473	0.0472	0.0465	0.0480	0.0480	0.0480

**Table 12.** 95% ACI and HPD (with their lengths) based on dataset I.

(n,m,k)	CS	$\nu$		$\eta$	
		ACI	HPD	ACI	HPD
(36,24,16)	A	(0.9451, 5.9792)	(1.1238, 5.6768)	(0.0287, 0.0450)	(0.0281, 0.0459)
		5.0341	4.5530	0.0162	0.0177
(36,28,20)	B	(1.6431, 8.3094)	(1.9056, 7.9251)	(0.0360, 0.0501)	(0.0355, 0.0510)
		6.6663	6.0195	0.0140	0.0155
(36,30,24)	C	(1.2922, 6.3808)	(1.4378, 6.0803)	(0.0390, 0.0555)	(0.0377, 0.0563)
		5.0887	4.6425	0.0165	0.0186

**Table 13.** Optimal censoring scheme under various criteria for generated sample based on dataset I.

Scheme	Criterion		
	I	II	III
A	<b>1.6492</b>	<b>2.752e-5</b>	59924
B	2.8918	3.523e-5	<b>82092</b>
C	1.6852	2.869e-05	58744

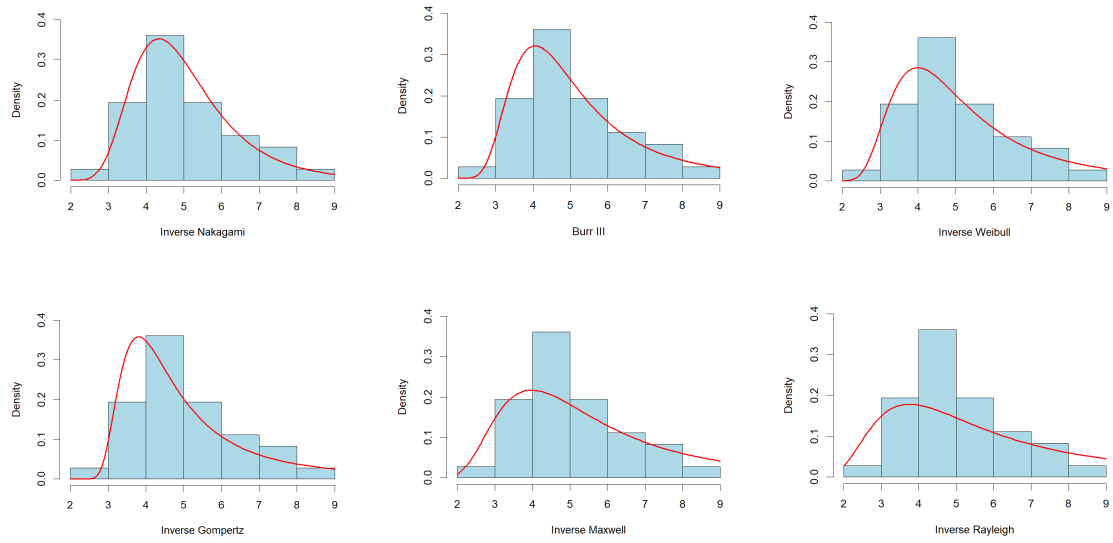


**Figure 4.** Histogram and density plots different models fitted to the dataset I.

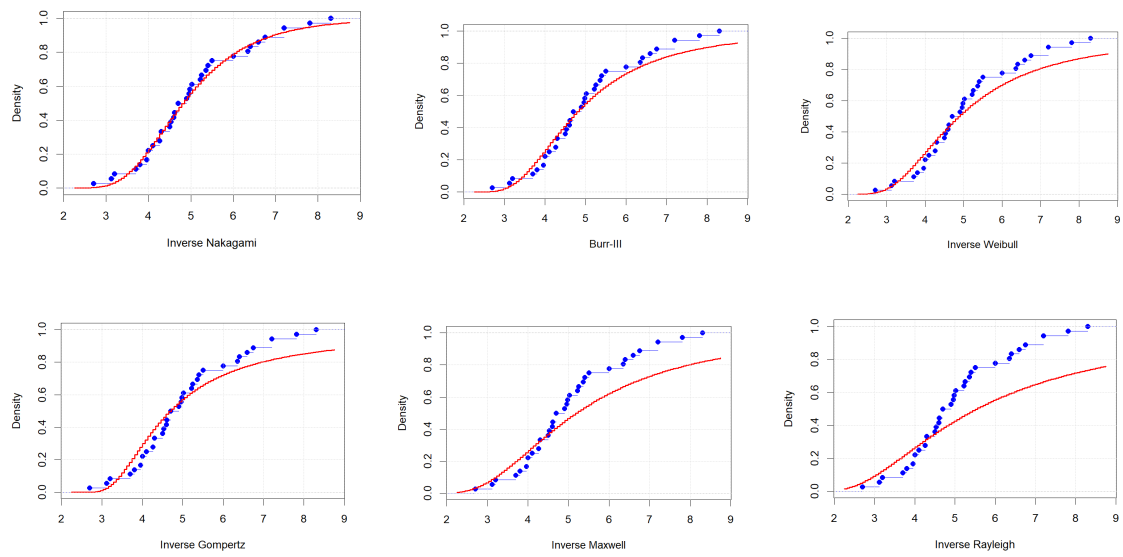


**Figure 5.** Empirical cdf and cdf plots for different models fitted to the dataset I.

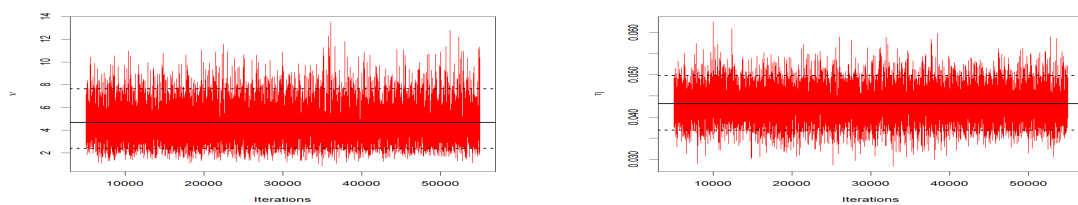


**Figure 6.** Trace plots of MCMC samples for  $\nu$  and  $\eta$  based on dataset I.

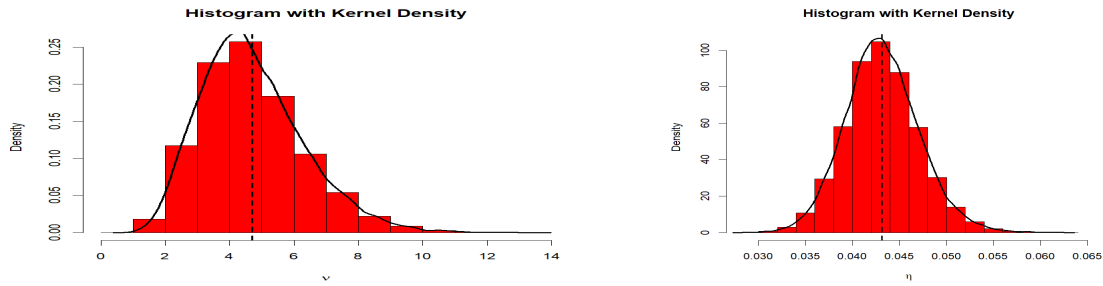


Figure 7. Histogram and kernel density plots of  $\nu$  and  $\eta$  based on dataset I.

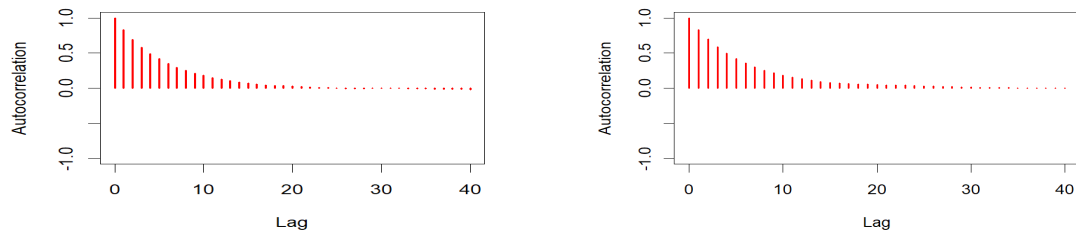


Figure 8. Autocorrelation plots of  $\nu$  (left) and  $\eta$  (right) based on dataset I.

Table 14. Three artificial UPHC schemes for dataset II.

$(n,m,k)$	Scheme	UPHC sample	$(T_1, T_2)$	D	R*	T*
$(40,20,16)$	$R = (20*1, 0*19)$	0.5, 2.5, 2.7, 3, 3, 3.3, 4, 4, 4.5, 4.7, 5, 5.4, 5.4, 7, 7.5, 8.8, 9, 10.2, 22, 24.5	$(5,10)$	16	4	8.8
$(40,24,20)$	$R = (8*1, 0*22, 8*1)$	0.5, 1, 1, 1, 1.1, 1.3, 1.5, 1.5, 1.5, 1.5, 2, 2, 2.2, 2.5, 2.7, 3, 3, 3.3 4, 4, 4.5, 4.7, 5, 5.4	$(3,5)$	20	12	4
$(40,30,24)$	$R = (0*29, 10*1)$	0.5, 0.6, 0.6, 0.7, 0.7, 0.7, 0.8, 0.8, 1, 1, 1, 1, 1.1, 1.3, 1.5, 1.5, 1.5, 1.5, 2, 2, 2.2, 2.5, 2.7, 3, 3, 3.3, 4, 4, 4.5	$(4,5)$	24	16	3

**Table 15.** Point estimates  $\nu$  and  $\eta$  (with their SEs) based on dataset II.

(n,m)	k	CS	Parameters	NR	EM	MAP	SELF	LLF	
								p = -0.25	p = 0.50
(40,20)	16	A	$\nu$	0.3001	0.3001	0.2729	0.2921	0.2923	0.2904
			$\eta$	0.2467	0.2465	0.2097	0.2856	0.2861	0.2812
(40,24)	20	B	$\nu$	0.3748	0.3748	0.3444	0.3642	0.3644	0.3617
			$\eta$	0.3670	0.3672	0.3365	0.3992	0.3996	0.3950
(40,30)	24	C	$\nu$	0.3712	0.3713	0.3461	0.3606	0.3609	0.3585
			$\eta$	0.6897	0.6895	0.6426	0.7494	0.7508	0.7368

**Table 16.** 95% ACI and HPD (with their lengths) based on dataset II.

(n,m,k)	CS	$\nu$		$\eta$	
		ACI	HPD	ACI	HPD
(40,20,16)	A	(0.1322, 0.4680)	(0.1402, 0.4577)	(0.0564, 0.4370)	(0.0998, 0.5426)
		0.3359	0.3175	0.3807	0.4427
(40,24,20)	B	(0.1720, 0.5776)	(0.1753, 0.5646)	(0.1630, 0.5711)	(0.1876, 0.6533)
		0.4057	0.3893	0.4081	0.4658
(40,30,24)	C	(0.1848, 0.5577)	(0.1894, 0.5427)	(0.3388, 1.0405)	(0.3814, 1.2048)
		0.3729	0.3533	0.7017	0.8234

**Table 17.** Optimal censoring scheme under various criteria for generated sample based on dataset II.

Scheme	Criterion		
	I	II	III
A	0.01677	6.912e-05	242.6
B	0.02155	1.159e-04	185.9
C	<b>0.0127</b>	<b>3.827e-05</b>	<b>332.3</b>

### 8. Conclusion

In this article, we have investigated the estimation problems of the inverse Nakagami-m distribution based on the unified progressive hybrid censored sample. The model parameters are estimated using the maximum likelihood method, implemented via the Newton-Raphson algorithm and the expectation-maximization (EM) algorithm. Bayesian estimates are obtained under gamma prior distributions using squared error and LINEX loss functions. Approximate confidence intervals for the unknown parameters are constructed on the basis of the asymptotic properties of the maximum-likelihood estimators (MLEs). To compute Bayesian estimates and construct the associated highest posterior density (HPD) credible intervals, the Markov Chain Monte Carlo (MCMC) approximation is employed. In addition, maximum a posteriori (MAP) estimates are evaluated.

Various diagnostic plots assess the convergence of the MCMC method. A comprehensive simulation study compares the performance of different estimation methods. The results indicate that Bayesian estimators outperform frequentist approaches in terms of bias, mean squared error (MSE), average confidence lengths (ACLs), and coverage probabilities (CPs). Furthermore, several optimality criteria determine the most suitable censoring scheme. Two real data sets are analyzed to demonstrate the practical applicability of the proposed methods. Based on the findings, the Bayesian MCMC approach is recommended for parameter estimation in the inverse Nakagami distribution under progressive hybrid

censoring.

**Conflicts of Interest:** There are no conflicts of interest with respect to the publication of this document.

**Author contributions.** All the co-authors have contributed equally in all aspects of the preparation of this submission.

**Conflict of interest statement.** The authors declare that they have no known competing financial interests or personal relationships that could have appeared to influence the work reported in this paper.

**Funding.** This research did not receive any specific grant from funding agencies in the public, commercial, or not-for-profit sectors.

**Data availability.** The data that support the findings of this study are openly available in [<https://doi.org/10.1080/02664763.2016.1258549>], reference number [11].

## References

- [1] A. Childs, B. Chandrasekar, N. Balakrishnan, and D. Kundu, *Exact likelihood inference based on Type-I and Type-II hybrid censored samples from the exponential distribution*, Ann. Inst. Stat. Math. **55**, 319-330, 2003.
- [2] A.I.E.S. Ibrahim, *On Estimation and Prediction for the Kumaraswamy Distribution Based on Progressive Censoring Schemes*. (Doctoral dissertation, Zagazig University) 2023.
- [3] A.P. Dempster, N.M. Laird and D.B. Rubin, *Maximum likelihood from incomplete data via the EM algorithm*, J. R. Stat. Soc. Ser. B Methodol. **39** (1), 1-22, 1977.
- [4] B. Chandrasekar, A. Childs and N. Balakrishnan *Exact likelihood inference for the exponential distribution under generalized Type I and Type II hybrid censoring*, Nav. Res. Logist. **51** (7), 994-1004, 2004.
- [5] B. Epstein, *Truncated life tests in the exponential case*, Ann. Math. Stat. 555-564, 1954.
- [6] B. Hasselman and M.B. Hasselman, *Package nleqslv*, R package version **3** (2), 2018.
- [7] B. Pradhan and D. Kundu, *Inference and optimal censoring schemes for progressively censored BirnbaumSaunders distribution*, J. Stat. Plan. Inference **143** (6), 1098-1108, 2013.
- [8] D. Kundu and A. Joarder, *Analysis of Type-II progressively hybrid censored data*, Comput. Stat. Data Anal. **50** (10), 2509-2528, 2006.
- [9] D. Kundu, *Bayesian inference and life testing plan for the Weibull distribution in presence of progressive censoring*, Technometrics **50** (2), 144-154, 2008.
- [10] F. Louzada, P. L. Ramos and D. Nascimento, *The inverse Nakagami-m distribution: A novel approach in reliability*, IEEE Trans. Reliab. **67** (3), 1030-1042, 2018.
- [11] H. Panahi, *Estimation of the Burr type III distribution with application in unified hybrid censored sample of fracture toughness*, J. Appl. Stat. **44** (14), 2575-2592, 2017.
- [12] M. Hashempour, *A new two-parameter lifetime distribution with flexible hazard rate function: Properties, applications and different method of estimations*, Math. Slovaca **71** (4), 983-1004, 2021.
- [13] J. Górný and E. Cramer, *Modularization of hybrid censoring schemes and its application to unified progressive hybrid censoring*, Metrika **81** (2), 173-210, 2018.

- [14] J. Bent. *Statistical properties of the generalized inverse Gaussian distribution* (Vol. 9). Springer Science & Business Media, 2008.
- [15] J. Kim and K. Lee, *Estimation of the Weibull distribution under unified progressive hybrid censored data*, J. Kor. Data Anal. Soc. **20**, 21892199, 2018.
- [16] K. Lee, H. Sun and Y. Cho, *Exact likelihood inference of the exponential parameter under generalized Type II progressive hybrid censoring*, J KOREAN STAT SOC. **45** (1), 123-136, 2016.
- [17] L. Wang, S. Dey and Y.M. Tripathi, *Classical and Bayesian inference of the inverse Nakagami distribution based on progressive Type-II censored samples*, Mathematics **10** (12), 2137, 2022.
- [18] M.H. Chen and Q.M. Shao, *Monte Carlo estimation of Bayesian credible and HPD intervals*, J. Comput. Graph. Stat. **8** (1), 69-92, 1999.
- [19] M. Irfan and A. K. Sharma, *Reliability characteristics of COVID-19 death rate using generalized progressive hybrid censored data*, Int. J. Qual. Reliab. Manag. **41** (3), 850-878, 2023.
- [20] G. S., Mohammad, *A new mixture of exponential and Weibull distributions: properties, estimation and reliability modelling*, São Paulo J. Math. Sci. **18** (1), 438-458, 2024.
- [21] M. Abramowitz and I. A. Stegun, (Eds.), *Handbook of mathematical functions with formulas, graphs, and mathematical tables (Vol. 55)*. US Government printing office, 1968.
- [22] M. Nakagami, *The m-distribution A general formula of intensity distribution of rapid fading*, In Statistical methods in radio wave propagation, 3-36, 1960. Pergamon.
- [23] M. Nassar and A. Elshahhat, *Estimation procedures and optimal censoring schemes for an improved adaptive progressively type-II censored Weibull distribution*, J. Appl. Stat. 1-25, 2023.
- [24] M. Plummer, N. Best, K. Cowles and K. Vines, *CODA: convergence diagnosis and output analysis for MCMC*, R news, **6** (1), 7-11, 2006.
- [25] M.H. Chen, Q.M. Shao and J.G. Ibrahim, *Monte Carlo methods in Bayesian computation*, Springer Science & Business Media, 2012.
- [26] N. Balakrishnan and R. Aggarwala, *Progressive censoring: theory, methods, and applications*, Springer Science & Business Media, 2000.
- [27] N. Balakrishnan, A. Rasouli and N. Sanjari Farsipour, *Exact likelihood inference based on an unified hybrid censored sample from the exponential distribution*, J. Stat. Comput. Simul. **78** (5), 475-488, 2008.
- [28] N. Metropolis, A.W. Rosenbluth, M.N. Rosenbluth, A.H. Teller and E. Teller, *Equation of state calculations by fast computing machines*, J. Chem. Phys. **21** (6), 1087-1092, 1953.
- [29] O.E. Abo-Kasem, A.R. El Saeed, and A.I. El Sayed, *Optimal sampling and statistical inferences for Kumaraswamy distribution under progressive Type-II censoring schemes*, Sci. Rep. **13** (1), 12063, 2023.
- [30] R.C.H. Cheng and N.A.K. Amin, *Estimating parameters in continuous univariate distributions with a shifted origin*, J. R. Stat. Soc. Ser. B Methodol. **45** (3), 394-403, 1983.
- [31] G. Shaheed, *Novel Weighted G family of Probability Distributions with Properties, Modelling and Different Methods of Estimation*, Stat. Optim. Inf. Comput. **10** (4), 1143-1161, 2022.
- [32] S.A. Lone, H. Panahi, S. Anwar and S. Shahab, *Estimations and optimal censoring schemes for the unified progressive hybrid gamma-mixed Rayleigh distribution*, Electron. Res. Arch. **31** (8), 4729-4752, 2023.

- [33] S. Dey, T. Dey and D.J. Lockett, *Statistical inference for the generalized inverted exponential distribution based on upper record values*, Math. Comput. Simul. **120**, 64-78, 2016.
- [34] S. Dutta and S. Kayal, *Estimation and prediction for Burr type III distribution based on unified progressive hybrid censoring scheme*, J. Appl. Stat. **51** (1), 1-33, 2024.
- [35] W.K. Hastings, *Monte Carlo sampling methods using Markov chains and their applications*, Biometrika **57**, 97-109, 1970.

## Appendix

The R code for sample generation and maximum likelihood estimation of unknown parameters of the inverse-Nakagami distribution under unified progressive hybrid censored sample is given below:

```

library(numDeriv)
library(Matrix)
library(rootSolve)
library(coda)
library(MCMCpack)
library(MASS)
library(nleqslv)
library(matlib)
library(zipfR)
library(Deriv)
library(nleqslv)
library(matlib)
library(zipfR)
n=50
m=40
T1 = 1
T2 = 2
k = 30
alpha = 1.5
beta = 2.5
lg= c()
z = c()
U=runif(n,0,1)
X1=array(0,m)
X=array(0,m)
t=array(0,m)
V=array(0,m)
Z=array(0,m)
#R=c(array(n-m,1), array(0,m-1)) # CS 1
#R = c(array(((n-m)/2), 1), array(0, (m-2)), array((n-m)/2, 1)) ## censoring 2
R=c(array(0,m-1),array(n-m,1)) ##cs 3
#R = c(array(1,5), array(0,m-6), array(n-m-5,1)) ## censoring

for(i in 1:m)
{
  t[i]=sum(R[(m-i+1):m])
}

```

```

for(i in 1:m)
{
  V[i]=U[i]^(1/(i+t[i]))
}
for(i in 1:m)
{
  Z[i]=1-prod(V[(m-i+1):m])
}
Data<-function(m,alpha,beta)
{
  u=runif(n, min = 0, max =1)
  library(zipfR)
  cdf = function(x,alpha,beta)
  {fn = (1/gamma(alpha))*(Igamma(alpha, (alpha/(beta*x^2)), lower =FALSE))}
  data=c() #Create an empty vector
  for(i in 1:m){
    fn<-function(x){cdf(x,alpha,beta)-Z[i]}
    uni<-uniroot(fn,c(0,100000))
    data=c(data,uni$root)}
  return(data)}
X = Data(m,alpha,beta)
if (X[m] < T1) {
  D = m;
} else if (X[k] < T1 && T1 < X[m]) {
  D = sum(X<T1);
} else if (T1 < X[k] && X[k] < T2) {
  D = k;
} else if (T2 < X[k]) {
  D = sum(X<T2);
} else {
  D =m
}

if (X[m] < T1) {
  Ts = X[m];
} else if (X[k] < T1 && T1 < X[m]) {
  Ts = T1;
} else if (T1 < X[k] && X[k] < T2) {
  Ts = X[k];
} else if (T2 < X[k]) {
  Ts = T2;
} else {
  Ts =X[m]
}

Rs = n-D-sum(R[1:D])
f = function(x){
  loglik = D*log(2/(gamma(x[1]))) +x[1]*D*log(x[1]/x[2]) -((2*x[1]+1)*sum(log(X[1:D]
  -loglik
}
G1=optim(c(alpha,beta),f,method="L-BFGS-B",lower=c(0.000001,0.000001), upper=c(Infi
A=sqrt(abs(diag(ginv(G1$hessian))))

```

```
v = ginv(G1$hessian)
ML=G1$par
ML
```